

Hard diffractive electroproduction of vector mesons in QCD

Leonid Frankfurt* and Werner Koepf†

School of Physics and Astronomy

Raymond and Beverly Sackler Faculty of Exact Sciences

Tel Aviv University, Tel Aviv, Israel

Mark Strikman‡

Pennsylvania State University, University Park, Pennsylvania

(Revised May 28, 1996)

in print by Phys. Rev. D

Abstract

Hard diffractive electroproduction of longitudinally polarized vector mesons is calculated within the leading $\alpha_s \ln \frac{Q^2}{\Lambda_{QCD}^2}$ approximation of QCD using the leading order parton densities within the nucleon. Novel QCD features of the production of excited states and of the restoration of flavor symmetry are analyzed. At the onset of the asymptotic regime, our analysis finds an important role of quark Fermi motion within the diffractively produced vector mesons, and we suggest to use this effect to measure the high momentum tail of the wave function of the vector mesons. We deduce a kinematical boundary for the region of applicability of the decomposition of the hard

*On leave of absence from the St.Petersburg Nuclear Physics Institute, Russia.

†Now at Ohio State University, Columbus, Ohio

‡Also St.Petersburg Nuclear Physics Institute, Russia.

amplitudes over powers of Q^2 and/or a limit on the increase of the cross sections of hard processes at small x , and briefly analyze its consequences. We also estimate the nuclear attenuation of the diffractive electroproduction of vector mesons and compare with estimates of the shadowing of the longitudinal structure function.

I. INTRODUCTION

Diffractive (coherent) production of hadron states in deep inelastic lepton-nucleon scattering is a new kind of hard process calculable in QCD. It provides the unique possibility to study the properties of vacuum exchange in QCD as well as the interplay between soft (nonperturbative) and hard (perturbative) contributions to the Pomeron. One of the main aims of such research is to obtain a three dimensional image of a hadron as compared to the one dimensional images extracted from the usual deep inelastic scattering off hadrons and nuclei. The idea to use diffractive electroproduction of vector mesons to investigate color coherence effects has been suggested many years ago in Refs. [1,2].

It has been shown in Ref. [3] that the cross sections of hard diffractive processes off a proton target are proportional to the square of the gluon distribution in the proton. Recently, Brodsky et al. [4] derived within the leading $\alpha_s \ln \frac{Q^2}{\Lambda_{QCD}^2} \ln \frac{1}{x}$ approximation a QCD prediction for the diffractive production of vector mesons built of light flavors in deep inelastic scattering. Diffractive photo- and electroproduction of J/Ψ mesons has been calculated by M.Ryskin [5] within the BFKL approximation of pQCD and within the charmonium constituent quark model approximation for the light-cone wave function of the J/Ψ meson.

On the experimental side, first HERA results on ρ -meson production at $Q^2 \geq 8 \text{ GeV}^2$ [6] and on photoproduction of J/Ψ mesons [7,8] have confirmed the fast increase of the cross section with energy predicted by pQCD.

In this paper, we extend the QCD analysis of Ref. [4] in several directions. We explain that the formulae of Ref. [4] are valid within the conventional leading $\alpha_s \ln \frac{Q^2}{\Lambda_{QCD}^2}$ approximation. So the cross section for hard diffractive electroproduction of vector mesons is expressed through the conventional leading $\ln \frac{Q^2}{\Lambda_{QCD}^2}$ order gluon distribution, and not by means of its asymptotics within leading order in $\alpha_s \ln \frac{Q^2}{\Lambda_{QCD}^2} \ln \frac{1}{x}$ as in Ref. [4]. This calculation justifies using the LO QCD improved parton model densities to compare QCD predictions for the electroproduction of vector mesons with experimental data.

We analyze the average transverse sizes of the $q\bar{q}$ components effective in $\sigma_{\gamma_L^* p}$, b_{σ_L} , and

in $\sigma_{\gamma_L^* p \rightarrow V p}$, $b_{\gamma_L^* \rightarrow V}$, and find them to decrease strongly with increasing Q^2 . At $Q^2 \sim 10$ GeV², those sizes are comparatively close, $b_{\sigma_L} \sim b_{\gamma_L^* \rightarrow V} \sim 0.3$ fm, while at larger Q^2 the rate of decrease of this average size is larger for b_{σ_L} . Thus we argue that the current $Q^2 \sim 10$ GeV² data suggest that the measured radius of the color distribution within a meson is $\sqrt{\frac{3}{2}} b_{\gamma_L^* \rightarrow V} \gtrsim 0.3 \div 0.4$ fm. This observation justifies the application of pQCD for the calculation of hard diffractive electroproduction of longitudinally polarized vector mesons. Really, the screening of the color charges insures the smallness of the effective interaction due to asymptotic freedom. In the case of $\sigma_{\gamma_T^* p}$, the effective transverse size of the $q\bar{q}$ components is expected to be intermediate between those in $\sigma_{\gamma_L^* p}$ and those in photoproduction because the contribution of soft QCD is enhanced for $\sigma_{\gamma_T^* p}$. Also, the significant difference between b_{σ_L} and $b_{\gamma_L^* \rightarrow V}$ indicates that substantial next-to-leading order corrections should be present in diffractive vector meson photo- and electroproduction which, in turn, should lead to a change of the scale effective in the gluon density.

We show that the QCD prediction for the Q^2 dependence of the ρ -meson production cross section is substantially weaker than that given by the naive dimensional estimate of $\sigma_{\gamma^* p \rightarrow V p}(x, Q^2) \propto Q^{-6}$ as a result of the increase of the parton distributions due to Q^2 evolution [9]. We find also a further slowing down of the Q^2 dependence due to the transverse quark motion in the vector mesons. Account of both effects resolves, to a large extent, seeming contradictions of predictions of Ref. [4] with the Q^2 dependence of the cross section of the ZEUS data [6]. Thus, investigation of the Q^2 dependence of the cross section of electroproduction of vector mesons may turn out to be an effective method to probe the three dimensional distribution of color in hadrons.

We analyze the energy and Q^2 dependence of the restoration of $SU(3)$ flavor symmetry in the electroproduction of vector mesons built of different flavors. We find that the ratio of the yields of ϕ - and ρ -meson production should increase with increasing Q^2 and/or $1/x$. We explain also that, in hard diffractive processes, $SU(4)$ flavor symmetry should be violated in the opposite way as compared to the low energy regime – production of heavy flavors should be enhanced at sufficiently large Q^2 . To analyze the onset of the restoration

of $SU(4)$ flavor symmetry, we evaluate diffractive photo- and electroproduction of J/Ψ and Ψ' mesons within the charmonium model approximation to the light-cone wave function of the J/Ψ and Ψ' mesons, as suggested in Ref. [5], and find that account of the quark Fermi motion leads to a significant additional suppression of J/Ψ photoproduction by a factor $\sim 1/8$ as compared to the asymptotic estimate, and to a slowing down of the onset of the asymptotic regime. Comparison with the data of Ref. [10,11,8,12] on J/Ψ photoproduction shows that the pQCD predictions can be brought to agree with the data within the uncertainties in the gluon distribution of a nucleon. We explain also that the charmonium models differ from QCD for large Q^2 . We furthermore present estimates for the yields of excited vector meson states in diffractive processes, $\gamma_L^* + p \rightarrow V' + p$. The interesting new effect, specific for QCD, is that the relative yield of excited states should increase with increasing $\frac{1}{x}$ and/or Q^2 .

Towards the end of the paper, we estimate the boundary of the kinematical region where, at very small x , the fast increase of the cross section with decreasing x should slow down and where existing methods of hard pQCD seem to be insufficient. We deduce the constraint on the kinematical range of applicability of the leading logarithm approximations and/or on the increase of the cross sections of hard processes with energy. We discuss practical consequences of this constraint and present model estimates for nuclear shadowing of the gluon distribution and of the diffractive vector meson electroproduction in interactions with heavy nuclei. These effects should be significant in kinematics which can be probed at colliding electron-nuclear beams at HERA and in the LHC heavy ion experiments.

Diffractive photo- and electroproduction of vector mesons has been investigated recently in Refs. [13–17] within the constituent quark model based on the two-gluon-exchange approximation [18]. Some of the predictions of that model – like the decrease of the effective size of the vector mesons with increasing Q^2 [13] or a significant production of ρ' mesons [14] – resemble results obtained in this paper. Other predictions – as the dip in the ρ' meson production at small Q^2 suggested in Ref. [14] or the qualitative difference

between the behavior of radial and orbital (e.g. D -state) excitations – do not follow from the QCD formulae of Ref. [4] and the current paper.

At the same time, we want to emphasize that at sufficiently large Q^2 , where a QCD calculation can be substantiated, the cross section should be expressed through the distribution of bare quarks in the vector meson and the parton distributions within the target [4] but not through the distribution of constituent quarks as in the models of Refs. [5,13–17]. There exists no direct relationship between the minimal Fock component of the light-cone hadron wave function, which enters in the QCD formulae for hard processes, and the wave functions of the constituent quark model. For example, the minimal Fock component of the quark-gluon wave function of vector mesons should decrease at large k_t^2 as a power of k_t^2 (cf. Ref. [19]) but not like a Gaussian as used in Refs. [13–17]. Just this difference is responsible for relevant effects found in the current work which are due to the transverse quark Fermi motion in the diffractively produced vector mesons. The qualitative difference between QCD calculations and the two-gluon-exchange model of Ref. [18] has been discussed in Ref. [4], and additional references to other works in that realm can also be found there.

The organization of this work is as follows: In Sect. II, we give leading $\alpha_s \ln \frac{Q^2}{\Lambda_{QCD}^2}$ predictions for the diffractive vector meson production in deep inelastic scattering, and, in Sect. III, we justify our pQCD approach listing the necessary approximations. In Sect. IV, we give estimates of the effects of transverse quark motion within the diffractively produced vector mesons and we discuss the NLO Q^2 rescaling. In Sect. V, we compare our results with the few currently available data. In Sect. VI, we discuss the restoration of flavor symmetry and, in Sect. VII, the production of excited states. In Sect. VIII, we estimate a kinematical constraint on the region of applicability of the leading logarithm approximations, and, in Sect. IX, nuclear shadowing in the hard diffractive production of vector mesons as well as the longitudinal structure function of a nucleus are considered.

II. LEADING $\alpha_S \ln \frac{Q^2}{\Lambda_{QCD}^2}$ PREDICTIONS FOR THE DIFFRACTIVE VECTOR MESON PRODUCTION IN DIS

It was demonstrated in Ref. [4], that a new kind of hard process, the coherent electro-production of vector mesons off a target T ,

$$\gamma^* + T \rightarrow V + T, \quad (1)$$

is calculable in QCD for $Q^2 \gg M_V^2$ within the leading $\alpha_s \ln \frac{Q^2}{\Lambda_{QCD}^2} \ln \frac{1}{x}$ approximation. Here, V denotes any vector meson ($\rho, \omega, \phi, J/\Psi$) or its excited states. For comparison with previous works and appropriate references see Ref. [4].

The idea behind the calculation of hard diffractive processes is that, when the coherence length, $l_c = \frac{1}{2m_N x}$, exceeds the diameter of the target, $2r_T$, the virtual photon transforms into a hadron component well before reaching the target and the final vector meson V is formed well past the target. The hadronic configuration of the final state is then the result of a coherent superposition of all those hadronic fluctuations, $|n\rangle$, in the photon wave function whose masses satisfy the condition:

$$- \frac{t_{min} r_T^2}{3} \ll 1. \quad (2)$$

Here, t_{min} is the minimal momentum transferred to the target:

$$- t_{min} = \left(\frac{M_n^2 + Q^2}{2q_0} \right)^2 = \left(1 + \frac{M_n^2}{Q^2} \right)^2 m_N^2 x^2. \quad (3)$$

Thus, as in the more familiar leading twist deep inelastic processes, the calculation should take into account all possible diffractively produced intermediate hadronic states satisfying Eq. (2). The use of completeness over those states allows us to express the result in terms of quark and gluon distributions, as in the case of other hard processes. The matrix element of electroproduction of a vector meson can thus be written as a convolution of the light-cone wave function of the photon, $\psi_{\gamma^* \rightarrow |n\rangle}$, the scattering amplitude of the hadron state, $A(nT)$, and the wave function of the vector meson, ψ_V :

$$A = \psi_{\gamma^* \rightarrow |n\rangle}^\dagger \otimes A(nT) \otimes \psi_V. \quad (4)$$

In the case of a longitudinally polarized photon with sufficiently large Q^2 , the sum over intermediate states $|n\rangle$ is a $q\bar{q}$ pair. This can be demonstrated by transition into impact parameter space and by showing that the essential distances, b , between the quarks in the wave function of the photon are $b^2 \propto 1/Q^2$. The situation is qualitatively different, however, for a transversely polarized photon due to the singular behavior of the vertex $\gamma_T^* \rightarrow q\bar{q}$ when one of the partons carries a small fraction of the photon momentum. In this case, soft and hard physics compete in a wide range of Q^2 and x .

Within the leading logarithmic approximation, i.e., $\alpha_s \ln \frac{Q^2}{\Lambda_{QCD}^2} \ln \frac{1}{x} \sim 1$, when terms of the order $\alpha_s \ln \frac{Q^2}{\Lambda_{QCD}^2}$ are neglected, the final result [4] for the cross section for the production of longitudinally polarized vector meson states, when the momentum transferred to the target t tends to zero, is¹

$$\left. \frac{d\sigma_{\gamma^* N \rightarrow VN}^L}{dt} \right|_{t=0} = \frac{12\pi^3 \Gamma_{V \rightarrow e^+e^-} M_V \alpha_s^2(Q) \eta_V^2 \left| \left(1 + i\frac{\pi}{2} \frac{d}{d \ln x}\right) x G_T(x, Q^2) \right|^2}{\alpha_{EM} Q^6 N_c^2}. \quad (5)$$

Here, $\Gamma_{V \rightarrow e^+e^-}$ is the decay width of the vector meson into an e^+e^- pair. The parameter η_V is defined as

$$\eta_V \equiv \frac{1 \int \frac{dz d^2 k_t}{z(1-z)} \Phi_V(z, k_t)}{2 \int dz d^2 k_t \Phi_V(z, k_t)}, \quad (6)$$

where Φ_V is the light-cone wave function of the $q\bar{q}$ component of the vector meson.

The factor $|\alpha_s(Q^2) x G_T(x, Q^2)|^2$ in Eq. (5) originates from the square of the cross section for the high-energy interaction of a small-size $q\bar{q}$ configuration with any target. It can be unambiguously calculated in QCD for low x processes by applying the QCD factorization theorem. In the approximation where only the leading $\alpha_s \ln \frac{Q^2}{\Lambda_{QCD}^2}$ terms are accounted for, the result is [21,22]

$$\sigma(b^2) = \frac{\pi^2}{3} \left[b^2 \alpha_s(Q^2) x G_T(x, Q^2) \right]_{x=Q^2/s, Q^2=\lambda/b^2}, \quad (7)$$

¹In Ref. [4], a factor 4 was missed in the numerator of Eq. (5) [20]. We are indebted to Z. Chan for pointing this out (A.Mueller private communication).

where b is the transverse distance between the quark q and the antiquark \bar{q} , $xG_T(x, Q^2)$ is the gluon distribution in the target, and $\lambda \approx 10$ according to our estimate in the next section. In this equation, the Q^2 evolution and small x physics are properly taken into account through the gluon distribution. $\sigma(b^2)$ can be inferred from the calculations of Ref. [23], which were performed in the leading $\alpha_s \ln x$ approximation of pQCD using certain input from hadronic quark models. Also, a quantity which can be related to $\sigma(b^2)$ has been calculated in Ref. [24] within the leading $\alpha_s \ln x$ approximation of pQCD while making specific assumptions on the parton structure of the constituent quarks.

The upper bound of the x -range of applicability of Eq. (5) is dictated by the condition that the formation time parameter should be much greater than the interaction time, which corresponds to the requirement that the longitudinal coherence length is larger than the target's diameter:

$$x \ll \frac{1}{4m_N r_T} \approx 0.06 . \quad (8)$$

Eqs. (5) and (7) can be easily generalized to the somewhat less restrictive leading $\alpha_s \ln \frac{Q^2}{\Lambda_{QCD}^2}$ approximation. Derivation of the respective formulae is relatively simple for hard diffractive processes initiated by longitudinally polarized photons because longitudinally polarized photons produce quarks in a PLC (point-like configuration) only. It can be demonstrated by transition into impact parameter space that the essential distances, b , between the quarks in the wave function of a longitudinally polarized photon with virtuality Q^2 are $b^2 \propto 1/Q^2$. Using b as the small parameter, it is easy to determine which Feynman diagrams dominate for the hard diffractive process. It is important to note that the integral over the distance between the quarks produced by the longitudinally polarized photon does not lead to terms proportional to $\ln b^2$ in the evaluation of the box diagrams. So the whole contribution is concentrated at small b . As a result, the factorization/decoupling theorem of QCD can be applied to factorize the hard part of the amplitude. So, to calculate the amplitude in the leading $\alpha_s \ln \frac{Q^2}{\Lambda_{QCD}^2}$ approximation, we need to accurately evaluate the hard blob and then convolute it with the parton distributions. The hard blob is described by the Feynman diagrams in Figs. 1a and 1b, where

gluons are attached to the quark box diagram.

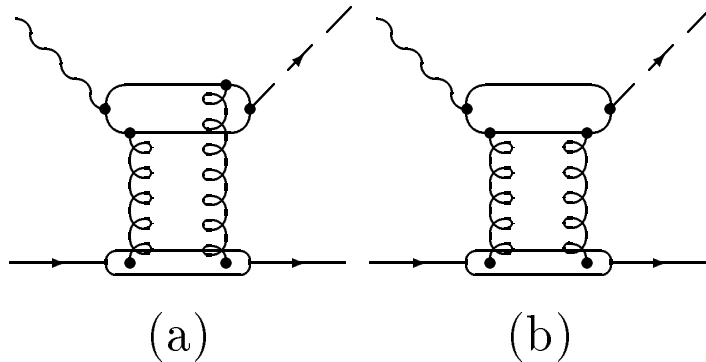


FIG. 1. Feynman diagrams relevant for the evaluation of the cross section of diffractive electroproduction of longitudinally polarized vector mesons, i.e., the $\gamma_L^* + T \rightarrow V + T$ process, in leading $\alpha_s \ln \frac{Q^2}{\Lambda_{QCD}^2}$ approximation.

Direct calculation of the sum of Feynman diagrams for the $\gamma_L^* \rightarrow V$ transition of Figs. 1a and 1b where only two gluons couple to the hard blob – although all interactions of these two gluons with the target are included – leads to seemingly the same formulae as in Ref. [4]. Really it is easy to demonstrate that within the leading $\alpha_s \ln b^2 \Lambda_{QCD}^2$ approximation, which is equivalent to the leading $\alpha_s \ln \frac{Q^2}{\Lambda_{QCD}^2}$ approximation, the dominant contribution is given by the diagrams with exchange of longitudinally polarized gluons. The diagrams corresponding to the exchange of transversely polarized gluons and those due to the quark sea in the nucleon are suppressed at small x . For a detailed discussion see Ref. [25].

The major difference from [4] is that, within the approximation discussed above, the full gluon distribution in the target calculated within the leading $\alpha_s \ln \frac{Q^2}{\Lambda_{QCD}^2}$ approximation should be used. In the formulae of Ref. [4], however, $xG_T(x, Q^2)$ is the gluon structure function calculated within the leading $\alpha_s \ln \frac{Q^2}{\Lambda_{QCD}^2} \ln \frac{1}{x}$ approximation. Remember, however, that corrections of powers $(lb)^n$ are numerically small and negative [4]. Here, l is the gluon's transverse momentum within the "pomeron".

In principle, the nondiagonal gluon distribution enters into those formulae. It will be explained in the next section that the usual parton distribution in the target T is a

reasonable approximation to this nondiagonal density. For a better understanding of the definition of the nondiagonal parton densities, these formulae should be compared to a similar one for the total photoabsorption cross section off a target T :

$$\sigma_{\gamma_L^* T} = \int_x^1 d\alpha G_T(\alpha, Q^2) \sigma_{\gamma_L^* g}(\alpha\nu, Q^2). \quad (9)$$

Eq. (9) is valid within the leading $\alpha_s \ln \frac{Q^2}{\Lambda_{QCD}^2}$ approximation, and the Q^2 evolution is contained in the Q^2 dependence of the parton distribution in the target T .

The analysis of the Feynman diagrams for $Im A_{\gamma_L^* T \rightarrow VT}$ shows that, for diffractive vector meson production, the region of integration over α is restricted as:

$$\alpha = x + \frac{M_{q\bar{q}}^2}{\nu}. \quad (10)$$

Here,

$$M_{q\bar{q}}^2 = \frac{m_q^2 + k_t^2}{z(1-z)} \quad (11)$$

is the invariant mass of the $q\bar{q}$ pair, and z and k_t define the light-cone momentum carried by the quark/antiquark in the wave function of the γ_L^* . The second term in Eq. (10) can be neglected for the production of vector mesons built of light quarks, since effectively $k_t^2 \ll Q^2$. This is because the wave function of the vector mesons decreases comparatively fastly with k_t^2 up to the onset of the pQCD regime. This explains why it is a reasonable approximation in $Im A_{\gamma_L^* T \rightarrow VT}$ – but not in Eq. (9) – to pull the parton densities at $\alpha \approx x$ out of the integrand.

The respective hard cross sections can be easily calculated through the minimal Fock components of the wave function of the vector meson. Thus, we deduce our asymptotic expression for the cross section of the electroproduction of vector mesons:

$$\left. \frac{d\sigma_{\gamma^* N \rightarrow VN}^L}{dt} \right|_{t=0} = \frac{12\pi^3 \Gamma_{V \rightarrow e^+e^-} M_V \alpha_s^2(Q) T(Q^2) \eta_V^2 \left| \left(1 + i\frac{\pi}{2} \frac{d}{d \ln x} \right) x G_T(x, Q^2) \right|^2}{\alpha_{EM} Q^6 N_c^2}. \quad (12)$$

The factor $T(Q^2)$ accounts for preasymptotic effects, i.e., $T(Q^2 \rightarrow \infty) = 1$, see the discussion in Sect. IV.

The major practical difference between the formulas deduced within the leading $\alpha_s \ln \frac{Q^2}{\Lambda_{QCD}^2} \ln \frac{1}{x}$ and the leading $\alpha_s \ln \frac{Q^2}{\Lambda_{QCD}^2}$ approximation (i.e., within the evolution equation) is that, in the leading $\alpha_s \ln \frac{Q^2}{\Lambda_{QCD}^2}$ approximation, $xG_T(x, Q^2)$ should be interpreted as the conventional parton distribution.

III. JUSTIFICATION OF THE PQCD APPROACH FOR DIFFRACTIVE VECTOR MESON ELECTROPRODUCTION IN DIS

The formal derivation of the pQCD expressions for the cross sections of hard diffractive processes in terms of the parton distributions in the target consists of several steps. The first is to demonstrate that, at small x , it is legitimate to use completeness over hadronic states to express the amplitude in terms of hard interactions of quarks and gluons. We discussed this in the previous subsection. The second step is to prove that the process is really hard and that it is legitimate to apply the QCD factorization theorem, and the third step is to show that the nondiagonal parton distributions of the target can be approximated through the conventional parton densities.

A. Applicability of pQCD and small transverse distances

To better understand the issue of applicability of pQCD to the process (1), it is convenient to perform the Fourier transform of the amplitude into the impact parameter space of the $q\bar{q}$ pair, which leads to

$$\mathcal{A}_{\gamma_L^* N \rightarrow V N} \propto \int d^2b dz \psi_{\gamma_L^*}^\dagger(z, b) \sigma(b^2) \psi_V(z, b). \quad (13)$$

Here, the Sudakov variable z denotes the fraction of the photon momentum carried by one of the quarks, b is the transverse distance between the quark and antiquark within the photon, and $\sigma(b^2) = \frac{\pi^2}{3} b^2 \alpha_s(b^2) xG_N(x, b^2)$ is the color-dipole cross section of Eq. (7) off a nucleon target. The advantages of the description of high energy processes in terms of light-cone wave functions of bound states in the impact parameter representation has

been understood long ago (cf. H.Cheng and T.T.Wu [26] and references therein). The $q\bar{q}$ component of the light-cone wave function of a longitudinally polarized virtual photon reads

$$\psi_{\gamma_L^*}(z, b) = 2Q z(1-z) K_0 \left(Qb\sqrt{z(1-z)} \right) \quad (14)$$

in the limit of vanishing quark mass, and where K_0 is the Hankel function of an imaginary argument.

To estimate which values of b dominate in the integral, in Eq. (13) we approximate $\psi_V(z, b)$ by

$$\psi_V(z, b) \propto z(1-z) \mu b K_1(\mu b) , \quad (15)$$

This form accounts for the common wisdom of the z dependence of the wave function of a longitudinally polarized vector meson, while the k_t dependence is chosen² to be $\propto \frac{1}{(k_t^2 + \mu^2)^2}$.

The parameter μ is related to the average transverse momentum of a quark/antiquark within the $q\bar{q}$ component of the meson's wave function through $\sqrt{\langle k_t^2 \rangle} = \mu/\sqrt{2}$. In our numerical analysis, we vary $\sqrt{\langle k_t^2 \rangle}$ between 300 and 600 MeV/c. Our guess is that, in reality, $\sqrt{\langle k_t^2 \rangle}$ should be of the order of $400 \div 500$ MeV/c, which is somewhat larger than the partons' average transverse momenta in hadrons. This is because, from the whole set of Fock components of the hadron wave function, the overlap with the wave function of the γ_L^* emphasizes the component which has no soft gluon field. An analysis of the energy denominators relevant for the wave functions of vector mesons shows that, in order to avoid a spurious pole, the $q\bar{q}$ component's energy denominator may dominate only in the kinematics

$$\frac{m_q^2 + k_t^2}{z(1-z)} \gg M_V^2 . \quad (16)$$

²In QCD, the expected behavior of $\propto \frac{1}{k_t^2}$ at large k_t corresponds to even smaller interquark distances in the wave function of the longitudinally polarized photon.

This condition is restrictive only for the minimal Fock space component. When the number of constituents is large, the energy denominator is large more or less automatically.

Now we need $\alpha_s(b^2)xG_N(x, b^2)$. We estimate it based on the impact parameter representation for $\sigma_L(x, Q^2)$,

$$\sigma_L(x, Q^2) = \int d^2b dz |\psi_{\gamma_L^*}(z, b)|^2 \sigma_{q\bar{q}N}(x, b) , \quad (17)$$

the nucleon's total longitudinal photoabsorption cross section, where

$$\sigma_{q\bar{q}N}(x, b) = \frac{\pi^2}{3} \alpha_s(Q^2) b^2 xG_N(x, Q^2) \Big|_{Q^2=\frac{\lambda}{b^2}} . \quad (18)$$

In the derivation of this equation, to simplify the estimates, we again pulled out the parton distributions in the mean point x .

We perform the analysis in two steps. First we use Eq. (18) and neglect the dependence of $\alpha_s(b^2) xG_N(x, b^2)$ on b^2 to estimate an average $b(Q)$ for this process. The latter we define as the value of b up to which we have to integrate to saturate 50% of the integral in Eq. (17). We then identify $G_N(x, b) \approx G_N(x, b(Q))$, determine a new average $b(Q)$, and then iterate this procedure to self-consistency. The final result of $b(Q)$ for $\sigma_L(x, Q^2)$ obtained in this manner is plotted as a solid curve in Fig. 2.

Thus, approximately $\lambda \approx 9.2$ or

$$G_N(x, b^2) \approx G_N \left(x, Q^2 = \frac{9.2}{b^2} \right) \quad (19)$$

for $x \sim 10^{-3}$. For fixed Q^2 , the transverse size $b(Q)$ slowly decreases with decreasing x : between $x = 10^{-3}$ and $x = 10^{-4}$ it drops by about 10%. The above reasoning accounts for some of the next to leading order $\alpha_s f \left(\alpha_s \ln \frac{Q^2}{\Lambda_{QCD}^2} \right)$ effects, based on the intuitive idea that the interaction is determined mostly by the spacial region occupied by color. Note that a numerically similar result was obtained by Nikolaev and Zakharov [28] in a consideration of F_L and $\partial F_T / \partial \ln Q^2$ ($\lambda \sim A_\sigma \approx 10$). However, in the derivation of the quantity A_σ in Ref. [28], the corresponding integrals were actually dominated by large b 's for which it is not clear whether the expression for the color-dipole cross section of Eq. (7) is at all applicable. Besides, no x -dependence of their A_σ was discussed in Ref. [28].

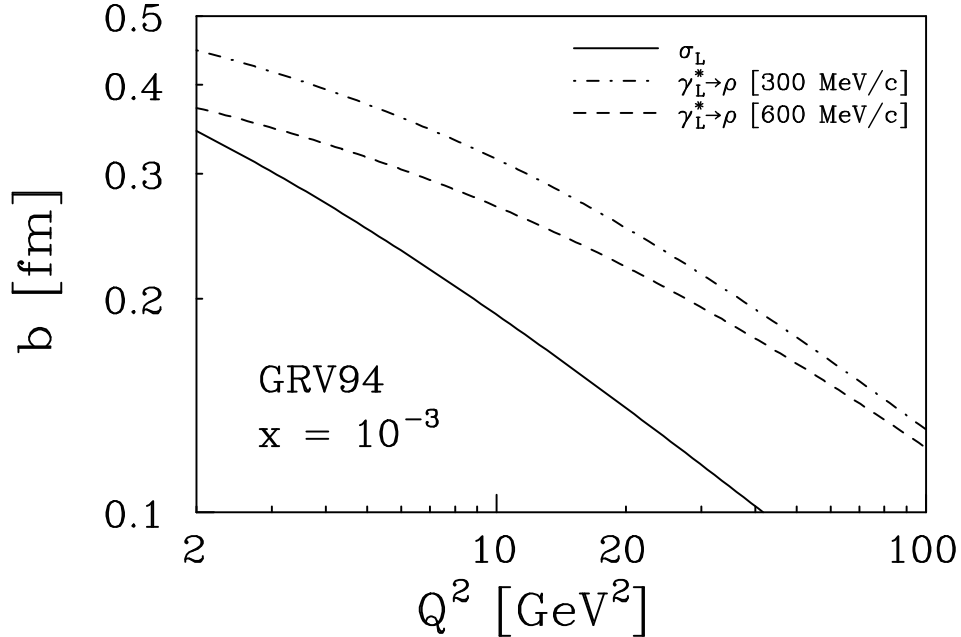


FIG. 2. Average transverse size of the $q\bar{q}$ components effective in $\mathcal{A}_{\gamma_L^* N \rightarrow V N}$ of Eq. (13) and σ_L of Eq. (17). In our numerical calculations, we used the GRV94 parametrization [27] of the nucleon's gluon density.

Then we use this value of $b(Q)$ to calculate the average transverse distances, $b_{\gamma_L^* \rightarrow \rho}(Q)$, relevant for longitudinal ρ -meson production. The results of such a calculation for $\sqrt{\langle k_t^2 \rangle} = 300$ and 600 MeV/c are presented also in Fig. 2. One can see that $b_{\gamma_L^* \rightarrow \rho}$ is quite small, however its numerical value is rather sensitive to the average value of $\sqrt{\langle k_t^2 \rangle}$. We observe also that $b_{\gamma_L^* \rightarrow \rho} > b_{\sigma_L}$. This difference may be rather small for $Q^2 \lesssim 10$ GeV 2 , but it becomes significant for $Q^2 \sim 100$ GeV 2 .

Note that the values we find for $b_{\gamma_L^* \rightarrow \rho}$ are substantially smaller than the typical distances between the valence quarks in a meson, $2r_M \sim 1.2$ fm. So, color is sufficiently screened within the wave function of the produced vector meson, and asymptotic freedom can be used to justify the applicability of pQCD for the calculation of diffractive electroproduction of ρ -mesons at $Q^2 \geq 10$ GeV 2 .

Our results for the elementary color-dipole cross section of a small size $q\bar{q}$ pair with a nucleon target, $\sigma_{q\bar{q}N}(x, b)$ of Eq. (18), are depicted in Fig. 3 for the GRV94 parametriza-

tion [27] of the nucleon’s gluon density and for various values of x . As expected, the cross section rises approximately quadratically with b and it increases dramatically with decreasing x . Note, however, that only for the smallest x , the cross section $\sigma_{q\bar{q}N}(x, b)$ approaches normal hadronic values ($\gtrsim 20$ mb). However, for such x , it reaches those already at quite small values of b , which, in turn, hints a limit of applicability of the leading logarithm approximations discussed here. This will be discussed further in Sect. VIII.

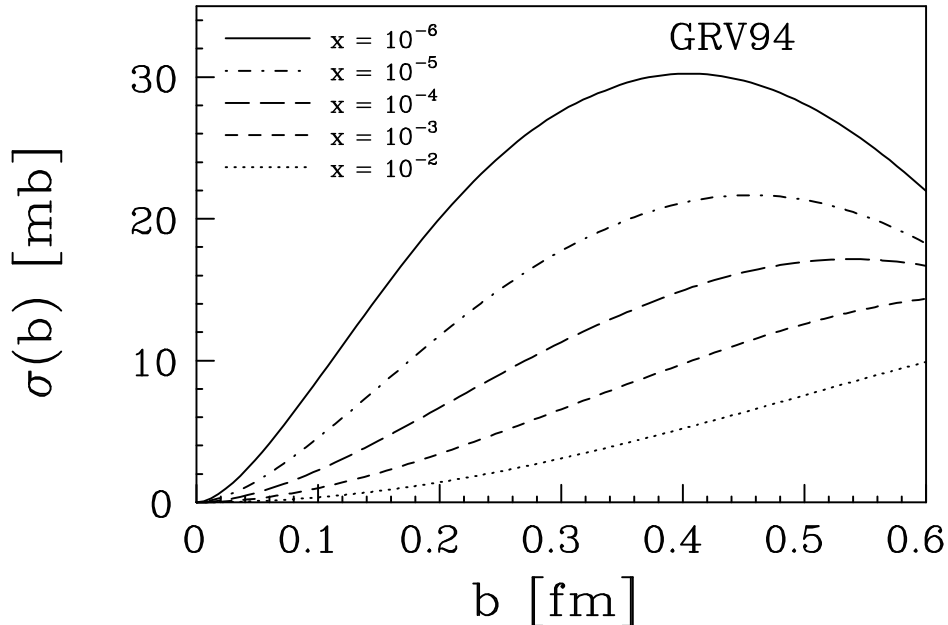


FIG. 3. Color-dipole cross section, $\sigma_{q\bar{q}N}(x, b)$ of Eq. (18), as a function of the transverse size of the $q\bar{q}$ pair for various values of x and for the GRV94 parametrization [27] of the nucleon’s gluon density.

Results for an analogous evaluation of the average transverse distances relevant for the photo- and electroproduction of charmonium mesons are depicted in Fig. 4. There, we employed nonrelativistic charmonium wave functions calculated from a power-law [29] and a logarithmic potential [30], which both describe $\Gamma_{J/\psi \rightarrow e^+e^-}$ reasonably well, and we set $z = \frac{1}{2} \left(1 + \frac{k_z}{m_c}\right)$. This yields $\psi_{\gamma^{(*)} \rightarrow c\bar{c}}(r) \propto \frac{e^{-\mu r}}{r}$, with $\mu = \sqrt{m_c^2 + \frac{Q^2}{4}}$, for the wave function of the $c\bar{c}$ component of the (virtual) photon. Note, however, that at sufficiently large Q^2 – which is the only domain at which the formulae for any vector meson production can

be consistently proven in QCD – $\int d^2k_t \psi_{J/\Psi}(k_t, z) \propto z(1-z)$ due to the Q^2 evolution [31,19], which is qualitatively different from the behavior expected for the nonrelativistic charmonium wave functions. The question which arises is thus whether hard physics is applicable at smaller Q^2 , and so we are effectively analyzing physics hidden under the assumption that the nonrelativistic charmonium wave functions approximate the light-cone wave function.

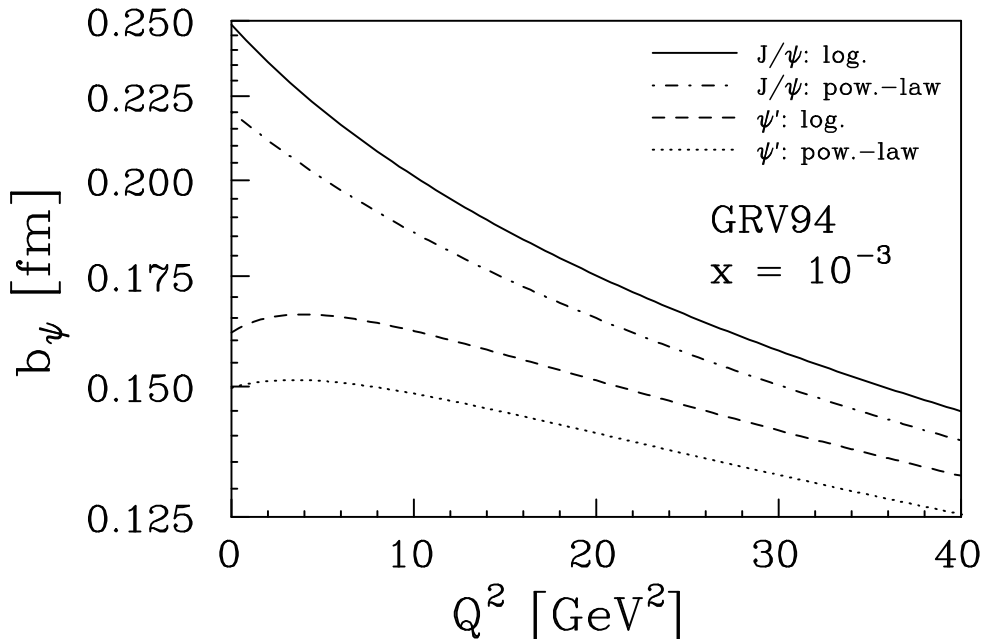


FIG. 4. Average transverse sizes of the $c\bar{c}$ components effective in $\mathcal{A}_{\gamma^{(*)}N \rightarrow V_c N}$ for J/Ψ and Ψ' photo- and electroproduction.

We observe that for J/Ψ photoproduction the corresponding relevant distances, b_Ψ , are similar to the average interquark distances in the J/Ψ mesons (~ 0.4 fm), while for the photoproduction of the excited state, the Ψ' , the distances that are most relevant for the photoproduction process are significantly smaller than the respective average interquark separations (~ 0.7 fm). Within the charmonium model approximation for the light-cone wave function of the Ψ' meson, this is due to the nodal structure of the wave function of the Ψ' , as was also observed by Benhar et al. [16] in the framework of the two-gluon-exchange model [18]. However, for charmonium electroproduction at larger Q^2 ,

the distances relevant in the amplitude are much smaller than the average interquark separations in the charmonium mesons.

We can now also estimate the contribution of the hard blob to the t dependence of the vector meson electroproduction cross section. In detail, we fit

$$\int d^2b dz \psi_{\gamma_L^*}(z, b) \sigma(b^2) \psi_V(z, b) e^{-iz\mathbf{p}_t\mathbf{b}} \propto e^{B_V t/2} \Big|_{t=-\mathbf{p}_t^2} \quad (20)$$

by an exponential at the vicinity of $t = 0$. The slope parameter that we find, $B_V \lesssim 0.7 \text{ GeV}^{-2}$, is much smaller than, e.g., the experimentally observed slope, $B_\rho = 4.6 \pm 0.8 \text{ GeV}^{-2}$ [32], of the ρ -production cross section off the nucleon. Hence, for all current practical considerations, the hard blob does not contribute significantly to the t dependence of the cross section, which hence originates almost entirely from the target's two-gluon form factor, $G_{2g}(t)$, and which is thus expected to be universal for all hard processes driven by the gluon density.

In the case of a transversely polarized γ^* , the contribution of large b , where nonperturbative QCD effects are dominant, is not suppressed. Those contributions arise from very asymmetric $q\bar{q}$ pairs with $z \sim 0$ or 1 [33,1,14], and, for transverse polarizations, in the integrand of the amplitude the regions z or $(1-z) \approx 1/Qb$ thus give important contributions, which are usually suppressed at large Q^2 by a Sudakov type form factor. In fact, it is easy to check that, for the case of transversely polarized photons, the contribution of this regions to the asymptotic expressions contains a logarithmic divergency. Hence, in this case, the integral over transverse momenta does not decouple.

On the other hand, the increase of $xG_N(x, b)$ at small x works towards enhancing the perturbative contribution of small b in this case as well. This is because the contribution of quark configurations with small b increases faster with decreasing x than the contribution from soft QCD. At what x and Q^2 the pQCD regime will dominate for reactions initiated by a γ_T^* is an open question since the contributions from soft QCD are not under control in this case. Currently, we are nevertheless estimating the hard, perturbative contribution to $\sigma_{\gamma_T^* N \rightarrow VN}$ [34].

Furthermore, since the formulae in this paper were deduced in the leading $\alpha_s \ln \frac{Q^2}{\Lambda_{QCD}^2}$

approximation only, there is an uncertainty in the theoretical formulae whether the gluon distributions should be evaluated at Q^2 or say at $Q^2/2$. A similar problem exists for calculations of the leading twist contribution to the total DIS cross section within the leading $\alpha_s \ln \frac{Q^2}{\Lambda_{QCD}^2}$ approximation. Note, also, that the substantial difference between $b_{\sigma_L}(Q^2)$ and $b_{\gamma_L^* \rightarrow V}(Q^2)$ which we found in this subsection indicates that significant next-to-leading order corrections should be present in diffractive vector meson photo- and electroproduction. We will give phenomenological estimates of these effects in Sects. IV.C and V.

B. The nondiagonal parton distributions

In this subsection, we show that the nondiagonal parton distributions of the target can be expressed through the diagonal – conventional – parton densities. The first observation is that the momentum transferred to the target, $t_{min} = -m_N^2 x^2 (1 + \frac{M_V^2}{Q^2})$, is negligible.

A more important issue is that the difference between the masses of the virtual photon and the vector meson leads to a difference between the light-cone fractions of the target momenta in the initial (x_i) and final (x_f) states. To elucidate this point, let us consider diffractive vector meson electroproduction in the center of mass of the $\gamma^* + T$ system. Suppose the initial target has momentum P . Kinematical considerations show that the final target has momentum $P(1 - (Q^2 + M_V^2)/s)$, and thus the difference between x_i and x_f is x [9].

For the hard part of the diffractive amplitude, the dependence on fractions of the target momentum carried by the interacting partons in the initial and final states is calculable in pQCD. This simplification arises since in the kinematics of diffractive processes, which dominate in the considered diagrams, it is legitimate to neglect in the propagators of the exchanged particles the contribution of the longitudinal part of their momenta as compared to the contribution of the transverse components. This can be easily proven within the $\alpha_s \ln \frac{Q^2}{\Lambda_{QCD}^2}$ and/or $\alpha_s \ln \frac{Q^2}{\Lambda_{QCD}^2} \ln \frac{1}{x}$ approximation by direct evaluation of the leading Feynman diagrams. In reality, this argument is valid beyond the pQCD regime

since it explores specifics of multipheripheral and multiregge kinematics.

Thus, we conclude that the initial and final parton wave functions of the target practically coincide, and it is a reasonable numerical approximation to use the diagonal parton densities. This question will be considered in detail in Ref. [25]. Here, we have explained that the tiny momentum transferred to the target does not influence the hard blob, which is specific for small x physics.

IV. ESTIMATES OF PREASYMPTOTIC EFFECTS

A. Vector mesons built of light quarks

The calculation discussed above is applicable at sufficiently large Q^2 , i.e., only when the transverse momenta in the $q\bar{q}$ pair are neglected, can the cross section for electroproduction of longitudinally polarized vector mesons be written in the form of Eq. (5). To analyze the onset of the asymptotic regime, we consider here the effects of the Fermi motion of the quarks within the diffractively produced vector meson. As originally suggested in Ref. [35], we do this by keeping the quarks' momenta in the propagator of the virtual photon, as the numerical coefficient which accompanies the leading term is large ($\approx \frac{32k_t^2}{Q^2}$). We will show that account of Fermi motion of the quarks within the vector meson leads to a significant suppression of the cross section at moderately large Q^2 . Thus, the formulae for diffractive electroproduction of vector mesons accounting for this Fermi motion contain an additional factor, $T(Q^2)$, which can be straightforwardly obtained from Eq. (2.15) of Ref. [4], and which, within the approximations discussed above, has the form:

$$T(Q^2) = \left(\frac{\int_0^1 dz \int_0^{Q^2} d^2 k_t \psi_V(z, k_t) \left(-\frac{1}{4} \Delta_t\right) \left[\frac{Q^4}{Q^2 + \frac{k_t^2 + m^2}{z(1-z)}} \right]}{\int_0^1 \frac{dz}{z(1-z)} \int_0^{Q^2} d^2 k_t \psi_V(z, k_t)} \right)^2. \quad (21)$$

Here, Δ_t is a two dimensional Laplace operator which acts on the wave function of the photon. We neglect here the current quark mass of the light quarks, which is small on the scale of the discussed phenomena.

To estimate the role of Fermi motion effects, we made estimates of the Q^2 dependence of T for three types of vector meson wave functions, $\psi_V(z, k_t) \sim z(1-z)\phi(k_t)$. For the nonperturbative piece, $\phi(k_t)$, we choose either $\phi(k_t) \propto \frac{1}{(k_t^2 + \mu^2)^2}$, as in the last section (labeled "dip."), or $\phi(k_t) \propto \exp(-k_t/\mu)$, as motivated by the observed transverse momentum distribution of direct pions in hadroproduction (labeled "exp."). We consider also a model where $\phi(k_t \geq 1\text{GeV}/c) \propto \frac{1}{k_t^2}$ (labeled "reg.") in order to check the sensitivity of our results on the large transverse momentum tail of the nonperturbative wave function. Such a behavior (without the naively expected $\alpha_s(k_t^2)$) follows directly from QCD [36]. At the same time, the region of applicability of the pQCD prediction for the high momentum tail, which we started at 1 GeV/c, is still subject of discussions. We then vary μ in the range corresponding to average transverse momenta $\sqrt{\langle k_t^2 \rangle} \sim 300 \div 600$ MeV/c. The results of these calculations are presented in Fig. 5.

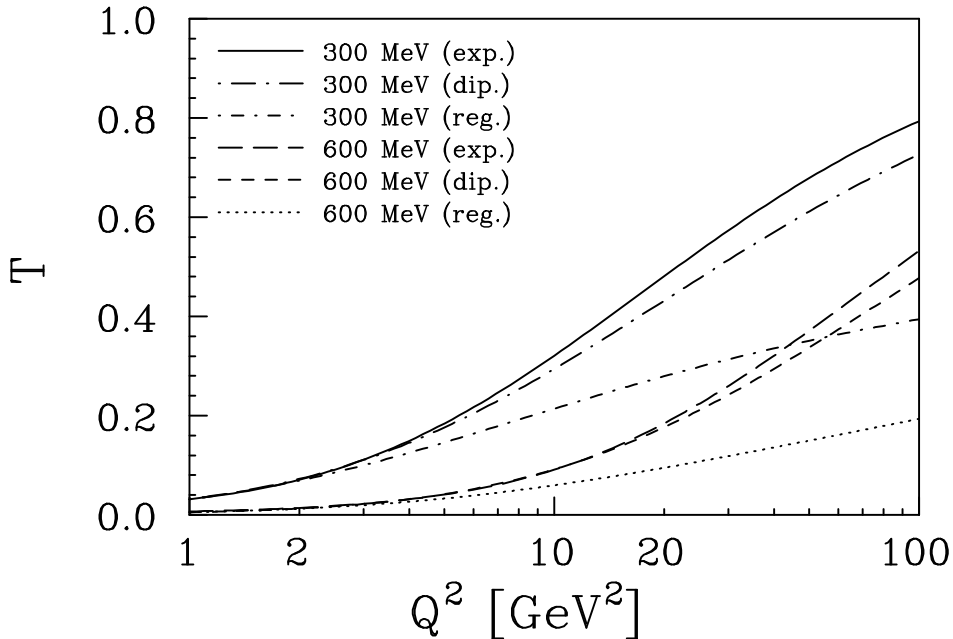


FIG. 5. Suppression factor, $T(Q^2)$ of Eq. (21), in $d\sigma_{\gamma_L^* N \rightarrow VN}/dt|_{t=0}$ due to transverse quark Fermi motion for diffractively produced vector mesons built of light quarks.

One can see that a very significant suppression of the vector meson yield may be present in the Q^2 range covered so far by the HERA experiments, and that the high momentum

tail – due to hard interactions between the constituents of the vector meson – seems to be an important correction in the relevant range of $Q^2 \gtrsim 10 \text{ GeV}^2$. As can be seen from Fig. 5, at large Q^2 , T is determined mostly by the high momentum tail of the k_t^2 distribution of the bare quarks within the diffractively produced vector meson. In mean field models of hadrons – bag models, constituent quark models with an oscillator potential or models based on the method of dispersion sum rules – this tail is included into the effective parameters, and thus these models give no clues for the value of this component, or its k_t and z dependence. On the other hand, as suggested by Fig. 5, a study of vector meson production over a wide range of Q^2 would allow to obtain unique information on the k_t distribution in hadrons. Note, however, that to achieve a nonambiguous interpretation of quark Fermi motion effects, it is necessary to calculate also the contribution of the $q\bar{q}g$ component in the light-cone wave functions of the γ_L^* and the vector meson to the cross section of hard diffractive processes. This has not been done so far.

B. Charmonium production

In the case of the photo- and electroproduction of heavy vector mesons, the overlap integral is suppressed both due to the presence of a term proportional to m_c^2 and due to quark Fermi motion.

To investigate the role of Fermi motion for a realistic case, we consider the non-relativistic model of charmonium. We keep terms proportional to $\frac{k^2}{m_c^2}$ in the wave function of the photon, as they enter with a large numerical coefficient and because the integral over the charmonium wave function only slowly converges at large momenta. At the same time, we neglect relativistic effects in the charmonium wave function and set³ $z \rightarrow \frac{1}{2} \left(1 + \frac{k_z}{\sqrt{k^2 + m_c^2}}\right)$. In this approximation, the phase volume in, for

³This formula follows from the necessity to transform light-cone perturbation theory diagrams into conventional, nonrelativistic diagrams describing the charmonium bound state.

instance, Eq. (21) becomes $\frac{dzd^2k_t}{z(1-z)} \rightarrow \frac{2}{\sqrt{k^2+m_c^2}}d^3k$, the energy denominator transforms into $\frac{m_c^2+k_t^2}{z(1-z)} \rightarrow 4(m_c^2+k^2)$, and the charmonium's light-cone wave function $\psi_V(z, k_t)$ can be obtained from its non-relativistic rest frame wave function $\psi_V(k)$ based on the requirement that the $J/\Psi \rightarrow e^+e^-$ decay width is reproduced correctly, which yields $\int dz d^2k_t \psi_V(z, k_t) = \int d^3k \psi_V(k)$. In this limit, $\eta_V \approx 2.44$, and the corresponding factor, F_V , is significantly smaller than unity:

$$F_V(Q^2) = \left(\frac{\int d^3k \psi_V(k) \left(-\frac{1}{16}\Delta_t\right) \left[\frac{Q^4}{Q^2 + \frac{k_t^2 + m_c^2}{z(1-z)}} \right]}{\int d^3k \psi_V(k) \frac{k^2 + m_c^2}{k_t^2 + m_c^2}} \right)^2. \quad (22)$$

Here, Δ_t is the two dimensional Laplace operator which acts on the wave function of the photon. For numerical estimates, we use two different realistic charmonium wave functions calculated from a QCD-motivated [37] and a logarithmic potential [30], which both describe $\Gamma_{J/\Psi \rightarrow e^+e^-}$ reasonably well. We hereby restrict our consideration to potential models for which the mass of the constituent c quark is close to the mass of the bare current c quark, i.e. $m_c \approx 1.5$ GeV ($m_c = 1.48$ GeV for the QCD-motivated potential of Ref. [37], and $m_c = 1.5$ GeV for the logarithmic potential of Ref. [30]). This is necessary to keep a minimal correspondence with the QCD formulae for hard diffractive processes which are expressed through the distribution of bare quarks [4]. The results of these calculations are shown in Fig. 6 for diffractive electroproduction of J/Ψ and Ψ' mesons, respectively. Fig. 6 shows that, in this model, the applicability of the asymptotic formulae requires rather large Q^2 .

Note that, in the evaluation of $\Gamma_{J/\Psi \rightarrow e^+e^-}$ and also in the process considered here, large radiative corrections, $1 - \frac{16\alpha_s(m_c^2)}{3\pi}$, accompany the charmonium's non-relativistic wave function but *not* the $q\bar{q}$ component of the light-cone wave function, which underlines the limits of applicability of non-relativistic charmonium potential models in that context. Inclusion of these radiative corrections effectively corresponds to a renormalization of the nonrelativistic wave function by the factor $1 - \frac{8\alpha_s(m_c^2)}{3\pi}$. Since we only employ the light-cone normalization of the wave function, this factor is implicitly included in all our calculations.

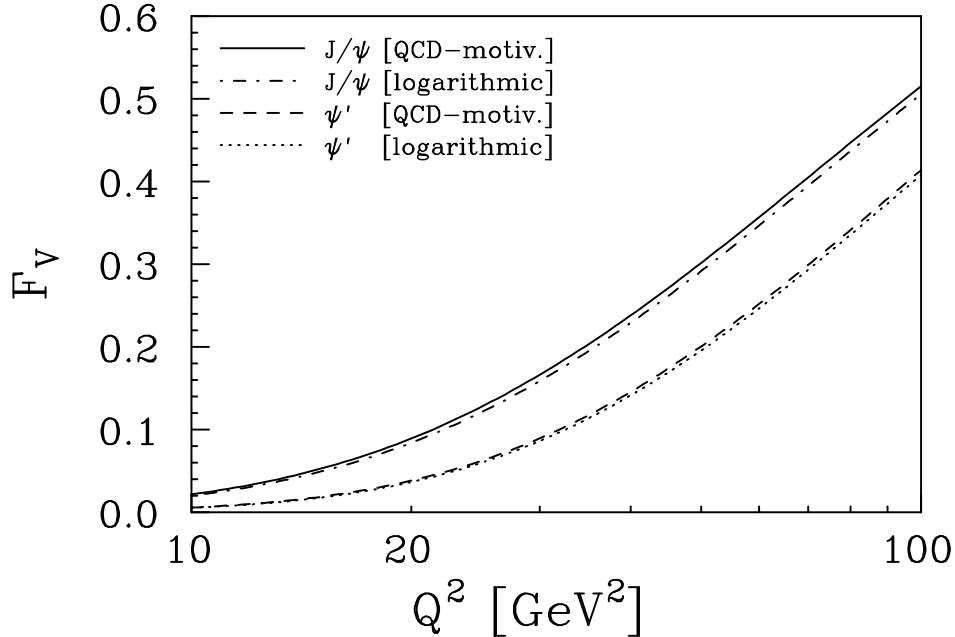


FIG. 6. Suppression factor, $F_V(Q^2)$ of Eq. (22), in $d\sigma_{\gamma_L^* N \rightarrow VN}/dt|_{t=0}$ due to the finite quark mass and quark Fermi motion for diffractively produced J/Ψ and Ψ' mesons.

Furthermore, the nonrelativistic charmonium model does not include gluon emission at higher resolution, and it therefore does not display the expected asymptotic behavior: $\int d^2k_t \psi_V(z, k_t) \propto z(1-z)$. In principle, this could be accounted for by means of b -space evolution of the leading twist wave function as suggested by Brodsky and Lepage [19].

In Ref. [5], pQCD was applied to the diffractive production of J/Ψ mesons starting from photoproduction. The observed increase of the J/Ψ photoproduction cross section with initial energy is in line with pQCD expectations [5]. Moreover, the theoretical analysis of the transverse distances between the c quarks within the J/Ψ meson shows that they are close to that dominant in the wave function of the γ^* in the deep inelastic structure functions. Thus, the necessary condition for the applicability of pQCD is the same in all cases. Specific to charmonium, however, is that these distances are close to the average distances between the quarks within the J/Ψ meson, as was discussed in the previous section. So, the process under consideration should be very sensitive to the exact form of the light-cone wave function of the J/Ψ meson and to its color field.

It was assumed in Ref. [5] that the cross section of diffractive J/Ψ electroproduction could be calculated employing the nonrelativistic constituent quark model for the J/Ψ meson's wave function, both for transverse and longitudinal photon polarizations, and quark Fermi motion was neglected. This corresponds to assuming that $R \equiv \eta_{J/\Psi} T_{J/\Psi} = 2$. In the limit where we can justify the application of pQCD ($M_{J/\Psi}^2 \ll Q^2$), our result coincides with that of Ref. [5] if we neglect Fermi motion and $m_c \neq M_{J/\Psi}/2$ effects, i.e., assume that $R = 2$, and if we discard the qualitative difference between the minimal $c\bar{c}$ Fock component in the J/Ψ 's wave function and its wave function in nonrelativistic potential models, which is actually not legitimate as was discussed in Sect. III.A. Thus, in Ref. [5], the predicted cross section is overestimated within the nonrelativistic quark model by a factor $T_V^{-1}(Q^2)$, where

$$T_V(Q^2) = \left(\frac{\int d^3k \psi_V(k) \left(-\frac{1}{16} \Delta_t\right) \left[\frac{(Q^2 + 4m_c^2)^2}{Q^2 + \frac{k_t^2 + m_c^2}{z(1-z)}} \right]}{\int d^3k \psi_V(k) \frac{k^2 + m_c^2}{k_t^2 + m_c^2}} \right)^2, \quad (23)$$

which is presented in Fig. 7 for the charmonium wave functions employed previously.

One can see from Fig. 7, that the effects of Fermi motion strongly suppress the contribution of the cross section, especially for $Q^2 \approx 0$ where most of the experimental data were obtained. If we evaluate the suppression factor T_V of Eq. (23) at the photoproduction point with charmonium wave functions calculated from the two nonrelativistic potentials of Refs. [30,37], we find a value of $T_V(Q^2 = 0) \approx 1/9$. This is significantly smaller than the corresponding value (~ 0.5) given recently by Ryskin et al. [38].⁴

⁴In our opinion, the reason for this discrepancy is threefold: Firstly, the authors of Ref. [38] use the approximate Fermi motion correction which we gave in Ref. [35], secondly they neglect the longitudinal relative motion of the quarks in the J/Ψ mesons – by setting $z = \frac{1}{2}$ – which, in turn, transforms the three dimensional integral over d^3k in Eq. (23) into a two dimensional integral over d^2k_t – see Eq. (23) in Ref. [38] – and, thirdly, a Gaussian form for the wave

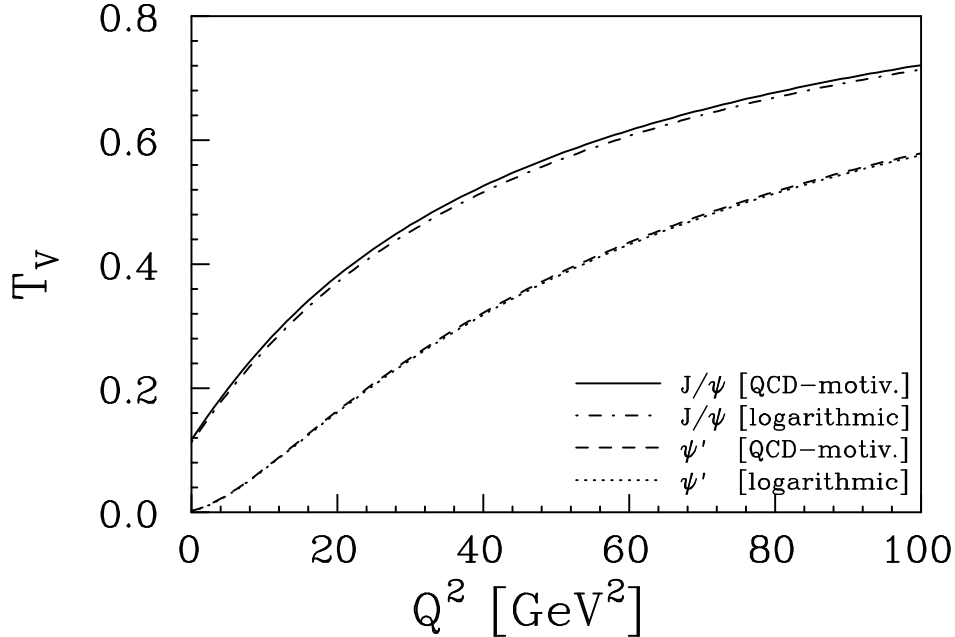


FIG. 7. Correction factor, $T_V(Q^2)$ of Eq. (23), in $d\sigma_{\gamma_L^* N \rightarrow VN}/dt|_{t=0}$ for diffractive charmonium production due to quark Fermi motion.

$T_V(0)$ has been evaluated also by decomposition over powers of $\frac{k^2}{m_c^2}$: $T_V(0) = 1 - \frac{20}{3} \langle \frac{k^2}{m_c^2} \rangle$. The difference between the actual number of $20/3$ and the 4 obtained in Ref. [38] is due to account of all terms arising from the application of the Δ_t operator. By definition, $\langle k^2 \rangle = \frac{\int k^2 \psi_V(k) d^3k}{\int \psi_V(k) d^3k}$. In Ref. [38], Gaussian type wave functions for the J/ψ were used to estimate that $\langle k^2/m_c^2 \rangle \approx 1/8$ (Note that for a pure Coulomb potential, which, when masked with a running coupling constant, corresponds to the limit $m_c \rightarrow \infty$ in QCD, $\langle k^2 \rangle = \infty$ due to

functions was assumed in Ref. [38], whereas the realistic potentials of Refs. [29,30,37] all yield wave functions that fall off significantly more slowly. All three approximations diminish the role of large quark momenta and result in an essential reduction of the suppression factor. For instance, our $T_V(Q^2 = 0)$ would rise from 0.11 to 0.4 if we were to use our approximate formula of Ref. [35] and change the integration over d^3k in Eq. (23) to an integration over d^2k_t , and it would rise further to 0.5 if we would replace our realistic charmonium wave functions with Gaussians. Note that the latter value coincides with that given in Ref. [38].

a linear divergency at large k). So, within this approximation, $T_V(0) \approx 1/(1 + \alpha_s)^6$.

The suppression factor $T_V(Q^2)$ has contributions from leading and non-leading twist. The respective leading twist expression follows from Eq. (21) by setting, in the wave function of the photon, k_t to zero after differentiation:

$$T_V^{LT}(Q^2) = \left(\frac{\int \frac{dz d^2 k_t}{z(1-z)} \psi_V(z, k_t) \left[\frac{(Q^2 + 4m_c^2)}{Q^2 + \frac{m_c^2}{z(1-z)}} \right]^2}{\int \frac{dz d^2 k_t}{z(1-z)} \psi_V(z, k_t)} \right)^2. \quad (24)$$

Additional (leading twist) terms containing $\ln m_c$ will be accounted for in a separate publication. Our analysis shows that, in QCD, the higher twist corrections are smaller, which, in turn, justifies our discussion of those Fermi motion effects in what is otherwise strictly a leading twist analysis.

Furthermore, the results of calculations of J/Ψ and Ψ' photoproduction cross sections are rather sensitive to the value used for the mass of the c quark, and, for instance, in Ref. [5] the assumption was made that $m_c = M_{J/\Psi}/2$. If we analyze the dependence of the J/Ψ photoproduction cross section on the difference between $M_{J/\Psi}$ and $2m_c$, we find a correction factor,

$$R_{M_{J/\Psi} \neq 2m_c} = \left(\frac{M_{J/\Psi}}{2m_c} \right)^6 \left(\frac{\int d^3 k \frac{\psi_V(k)}{(1+k^2/m_c^2)^2} \frac{k^2+m_c^2}{k_t^2+m_c^2}}{\int d^3 k \frac{\psi_V(k)}{(1+4k^2/M_{J/\Psi}^2)^2} \frac{k^2+m_c^2}{k_t^2+m_c^2}} \right)^2, \quad (25)$$

which, using the values for m_c and the respective charmonium wave functions from Refs. [30,37], yields $R_{M_{J/\Psi} \neq 2m_c} \approx 1.2$. This, together with our $T_V(Q^2 = 0)$, gives a final prediction for the suppression of J/Ψ photoproduction of⁵ $\approx 1/8$.

⁵In Ref. [38], the correction factor of Eq. (25) was approximated by $(M_{J/\Psi}/2m_c)^8$, and the latter was evaluated with a small $m_c = 1.43$ GeV, as estimated by Jung et al. [39], which, in turn, yields a very strong enhancement of $R_{M_{J/\Psi} \neq 2m_c} \approx 2$. This estimate is at variance with the direct calculation using Eq. (25). This, together with the underestimated Fermi motion

C. Q^2 rescaling

In Sect. III.A, we determined the relevant transverse distances between the quark and the antiquark in the hard blob of Fig. 1, and we found that they depend on the process under consideration, i.e. there is a substantial difference between $b_{\sigma_L}(Q^2)$ and $b_{\gamma_L^* \rightarrow V}(Q^2)$.

In detail, we used the impact parameter representation of the longitudinal structure function, $\sigma_L(x, Q^2)$ of Eq. (18), to define a relation between the transverse size of the $q\bar{q}$ pair, b , and the virtuality of the process, Q^2 . This relation,

$$b = b_{\sigma_L}(Q^2) \approx \frac{9.2}{Q^2}, \quad (26)$$

at $x = 10^{-3}$, yields the scale effective in the gluon densities which enter, for instance, in the elementary color-dipole cross section, $\sigma(b^2)$ of Eq. (7). It is designed in such a way that, if we were to evaluate the integrand of Eq. (18) at this average $b = b_{\sigma_L}(Q^2)$ instead of carrying out the integral, we would just recover the normalization condition: $\sigma_L(x, Q^2) \propto \alpha_s(Q^2) xG_N(x, Q^2)$. Hence, the virtuality that corresponds to the dominant transverse distances and the virtuality of the process are identical, at least for the case of the longitudinal photoabsorption cross section.

However, this is not the case for the electroproduction amplitude, $\mathcal{A}_{\gamma_L^* N \rightarrow V N}$ of Eq. (13), due to the significant difference between the transverse distances it is dominated by and $b_{\sigma_L}(Q^2)$. This indicates that substantial next-to-leading order corrections should be present in diffractive vector meson photo- and electroproduction which, in turn, should lead to a change of the scale effective in the gluon densities, i.e., the virtualities that enter in the argument of $\alpha_s(Q^2) xG_N(x, Q^2)$ in our basic equation (12).

Following our logic of approximating the integrals over the transverse sizes of the $q\bar{q}$ pair effective in the hard blob of Fig. 1 by the contribution from an appropriately defined

correction, leads the authors of Ref. [38] to the conclusion that there is no net suppression for J/Ψ photoproduction.

average transverse distance, a natural guess is to rescale the virtuality Q^2 in proportion of these average transverse sizes,

$$Q_{eff}^2 \approx Q^2 \frac{b_{\sigma_L}^2(Q^2)}{b_{\gamma_L^* \rightarrow \rho}^2(Q^2)}, \quad (27)$$

which, for ρ production, yields significantly smaller virtualities, i.e., $Q_{eff}^2 < Q^2$. This results in a strong decrease of the quantity $[\alpha_s(Q^2) xG_N(x, Q^2)]^2$, and therefore also of the ρ -meson electroproduction cross section, as can be seen in Fig. 8 where we show $[\alpha_s(Q^2) xG_N(x, Q^2)]^2$ with and without the NLO rescaling.⁶

In Fig. 8, we also plot the exponent of the energy dependence of $[\alpha_s(Q^2) xG_N(x, Q^2)]^2$ (and hence of the predicted cross sections), $m_x(Q^2)$, which is defined by means of $[\alpha_s(Q^2) xG_N(x, Q^2)]^2 \propto x^{-m_x(Q^2)}$. We observe that the rescaling not only significantly reduces the predicted cross sections, but it also results in a slight reduction of its steep energy dependence.

On the other hand, the relevant transverse distances for J/Ψ photoproduction, $b_{J/\Psi}(Q^2 = 0)$, are relatively small, $b_{J/\Psi}(Q^2 = 0) \approx 0.25$ fm, which, using the logic outlined in the above, results in substantially higher effective virtualities, $\overline{Q}^2 \approx \frac{9.2}{b_{J/\Psi}^2} \approx 5.1$ GeV², for J/Ψ photoproduction than those suggested, for instance, in Ref. [38] – $\overline{Q}^2 = 2.4$ GeV². This will be discussed in more detail in Sect. V.C.

In Fig. 9, we finally show the Q_{eff}^2 obtained in this manner for the cases of ρ -meson electroproduction and J/Ψ photo- and electroproduction. Note that the relationship between Q^2 and Q_{eff}^2 is almost independent of x , and that the Q_{eff}^2 for J/Ψ production differs significantly from the estimate of Ref. [38], $\overline{Q}^2 = \frac{Q^2 + M_{J/\Psi}^2}{4}$, which is shown through the dotted line in Fig. 9b.

⁶Eq. (27) assumes that $G_N(x, Q^2)$ is defined such that Eq. (9) for σ_L is valid in the NLO approximation. This question requires further investigation. However, the corresponding uncertainty is numerically unimportant for the comparison of production rates of different vector mesons.

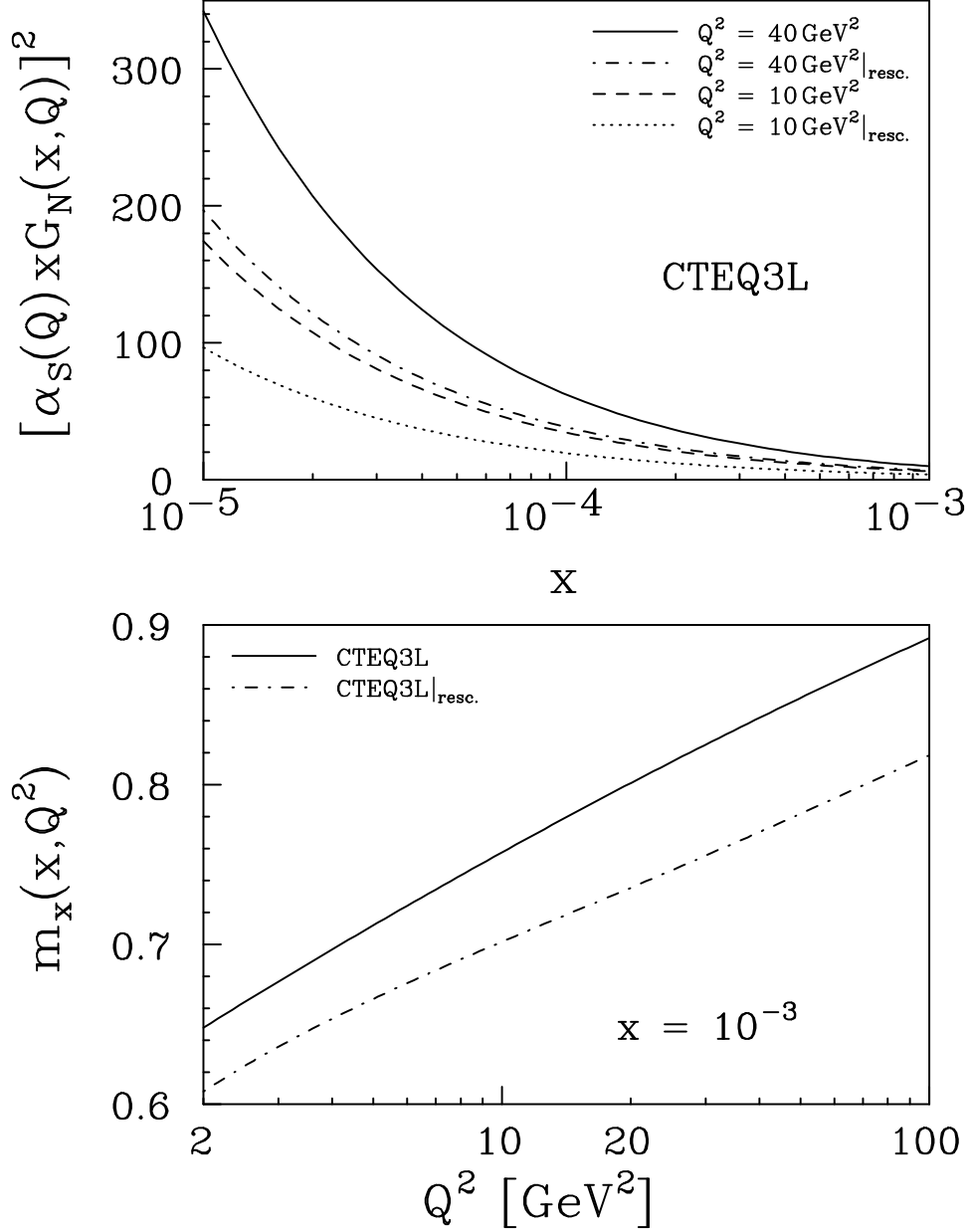


FIG. 8. The square of the gluon density, $[\alpha_s(Q^2) x G_N(x, Q^2)]^2$, and its energy dependence, $m_x(Q^2)$, defined by $[\alpha_s(Q^2) x G_N(x, Q^2)]^2 \propto x^{-m_x(Q^2)}$ calculated for the CTEQ3L parton distribution function with and without the NLO (ρ -meson electroproduction) rescaling introduced in Eq. (27).

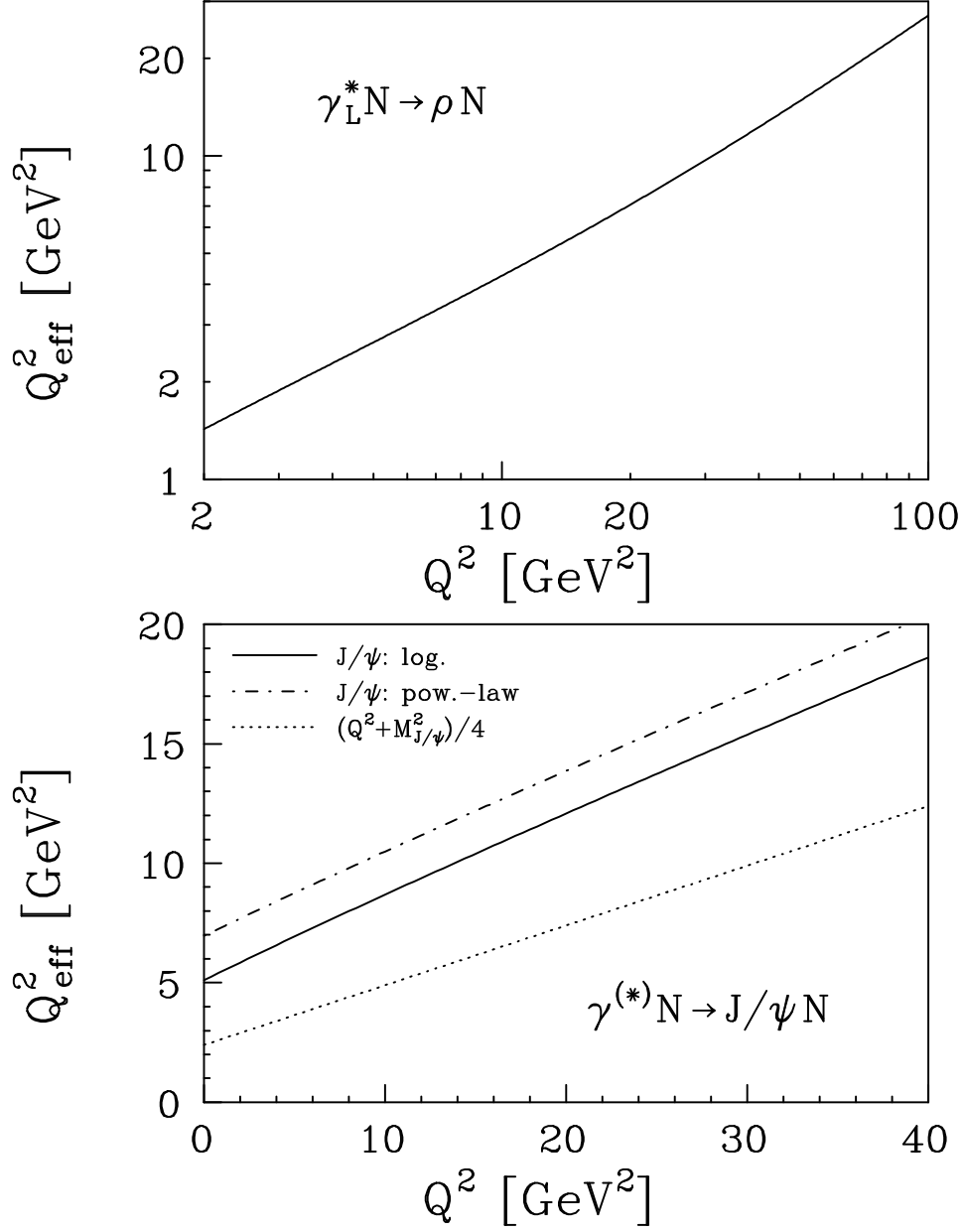


FIG. 9. Q_{eff}^2 obtained via the NLO Q^2 rescaling introduced in Eq. (27) for ρ -meson electroproduction and J/Ψ photo- and electroproduction. For the latter, we also show the estimate of Ref. [38] (the dotted line).

V. COMPARISON WITH DATA

A. Main features of the data

The HERA data [6], when combined with the NMC data [32] on diffractive electroproduction of ρ -mesons, are consistent with several key predictions of Eq. (12):

(i) a fast increase with energy of the cross section for electroproduction of vector mesons, which is approximately proportional to $x^{-0.6}$ for $Q^2 = 10 \text{ GeV}^2$. Note that this fast increase with decreasing x is not expected within the non-perturbative two-gluon-exchange model of Donnachie and Landshoff [40], which predicts a cross section rising as $\sim x^{-0.16}$ at $t = 0$, and an even weaker increase of the cross section when integrated over t due to a substantial increase of the slope of the elastic cross section expected in soft Pomeron models: $\sigma_{el} \propto \frac{1}{x^{0.16}} \frac{B_0}{B_0 + 2\alpha' \ln \frac{x_0}{x}}$. Here, B_0 is the slope of the elastic cross section for $x = x_0$.

(ii) the dominance of the longitudinal polarization, $\frac{\sigma_L}{\sigma_T} \propto Q^2$ [4,40]. Data do confirm the dominance of σ_L , though they are not accurate enough to study details of the Q^2 dependence. Predictions for the x -dependence of this ratio sensitively depend on the interplay of perturbative and nonperturbative contributions to σ_T . In the leading $\alpha_s \ln \frac{Q^2}{\lambda_{QCD}^2}$ approximation, it is easy to generalize the QCD evolution equation to transversely polarized photons as a projectile [9]. As in the case of the regular structure functions, the appropriate question will be on the region of integration over fractions of momenta appropriate to the hard blob. Since the hard kernel in the evolution equation increases faster at small x than the soft contribution, one may expect an onset of hard physics for transversely polarized photon projectiles as well, though at smaller x and at higher Q^2 . Note that at sufficiently large Q^2 , the contribution of nonperturbative QCD to diffractive vector meson production is suppressed in addition by a Sudakov type form factor. At sufficiently large Q^2 , the process should be discussed in terms of the Bethe-Salpeter wave function for the transition of a ρ -meson into two highly virtual quarks. Such a mathematical object exists in pQCD only. Thus, there exists a possibility to check quark counting rules in their

original form. This may manifest itself in the x -dependence of the ratio $\frac{\sigma_L}{\sigma_T}$ for fixed Q^2 . At intermediate $Q^2 \sim 10 \text{ GeV}^2$, where hard physics already dominates in σ_L , σ_T may still be determined by soft, nonperturbative contributions. For these Q^2 , the ratio should increase with decreasing x as $x^2 G_N^2(x, Q^2)$. At high Q^2 , where hard physics dominates for both σ_L and σ_T , the ratio would not depend on x . We are currently investigating these issues in detail [34]. The x dependence of $\frac{\sigma_L}{\sigma_T}$ was also discussed in Ref. [15]. The authors employed nonrelativistic oscillator wave functions for the diffractively produced vector mesons, and the pQCD color-dipole picture was applied for both polarizations and also for large transverse distances. For both cases, the formula for the elementary color-dipole cross section, $\sigma(b^2)$ of Eq. (7) which was deduced in [21,22], is clearly not applicable, as was discussed in detail in Sect. III.

(iii) the absolute magnitude of the cross section is reasonably well explained, though uncertainties in the knowledge of $xG_N(x, Q^2)$ are rather large to make a comparison quantitative. This will be discussed in detail in the next subsection.

(iv) the Q^2 dependence observed by the ZEUS collaboration: $\sigma_L \propto Q^{-n}$ with $n = 4.2 \pm 0.8$ [6]. This seems to reflect the Q^2 evolution of the parton distributions as well as effects of quark Fermi motion within the vector mesons, as will be outlined in subsection V.D.

B. Absolute magnitude of the ρ -electroproduction cross section

Currently, absolute cross sections for exclusive ρ -meson production are available from NMC [32] and from ZEUS [6].

We restrict our analysis here to $Q^2 \geq 6 \text{ GeV}^2$. In the case of NMC, the most relevant data are those obtained using a deuteron target as no data were taken with hydrogen. The measurements do not separate the elastic deuteron final state and deuteron break up. So, to extract the cross section for ρ -production off the nucleon from the deuteron data, we use the closure approximation to sum over the final states of the two nucleons, which yields [41]

$$\frac{d\sigma_{\gamma^*D\rightarrow\rho D}}{dt} = 2(1 + F_D(4t))\frac{d\sigma_{\gamma^*N\rightarrow\rho N}}{dt}, \quad (28)$$

where $F_D(t)$ is the deuteron's electromagnetic form factor. In the above, we neglected shadowing, Glauber rescattering effects (which are suppressed due to color transparency expected in this kinematics) and the real part of the elementary amplitude. $F_D(t)$ can be roughly parameterized as $F_D(t) \sim e^{B_D t}$ with $B_D \approx 14 \text{ GeV}^{-2}$ [41]. This yields

$$\sigma_{\gamma^*N\rightarrow\rho N} = \frac{\sigma_{\gamma^*D\rightarrow\rho D}}{2} \left(1 - \frac{B}{4B_D}\right), \quad (29)$$

where $B = 4.6 \pm 0.8 \text{ GeV}^{-2}$ [32] is the slope of the ρ -production cross section off the nucleon. With this, the total cross section of ρ -production on the nucleon, $\sigma_{\gamma^*N\rightarrow\rho N}$, can be calculated from the NMC's deuteron data. Using their determination of the virtual photon's polarization, $\langle\epsilon\rangle$, and the measurement of $R = \sigma_{\gamma^*N\rightarrow\rho N}^L/\sigma_{\gamma^*N\rightarrow\rho N}^T = 2.0 \pm 0.3$ at $\langle Q^2 \rangle = 6 \text{ GeV}^2$, we can furthermore separately extract the elementary longitudinal cross section, $\sigma_{\gamma^*N\rightarrow\rho N}^L$. In the same manner, $\sigma_{\gamma^*N\rightarrow\rho N}^L$ can be obtained from the ZEUS data where $R = 1.5 \pm 0.6$ (statistical errors only) at $\langle Q^2 \rangle = 11 \text{ GeV}^2$.

Results of such calculations are presented in Fig. 10. There, we also show theoretical predictions of Eq. (12) employing several recent parametrizations of the gluon density⁷ [42,43,27] and typical parameters for the ρ -meson wave functions as considered in section IV. We set $\eta_V = 3$ and parametrize the dependence of the differential cross section on the momentum transfer in exponential form with⁸ $B \approx 4 \text{ GeV}^{-2}$. Note that a change of $T(Q^2)$ in the range depicted in Fig. 5 introduces an extra scale uncertainty of $0.5 \div 2$.

⁷Note that, within the leading $\ln \frac{Q^2}{\Lambda_{QCD}^2}$ approximation to QCD, the use of NLO fits to the nucleon's gluon density is not fully consistent.

⁸A natural estimate for B is $B = \frac{\langle r_g^2 \rangle}{3} + B_{\gamma_L^* \rho}(Q^2)$ where $\sqrt{\langle r_g^2 \rangle}$ is the mean radius of the gluon distribution in a nucleon which is usually taken in realistic models of the nucleon as 0.6 fm. The calculation of Sect. III.A gives $B_{\gamma_L^* \rho}(Q^2) \approx 0.7 \text{ GeV}^{-2}$. Putting all numbers together we obtain $B \approx 3.8 \text{ GeV}^{-2}$.

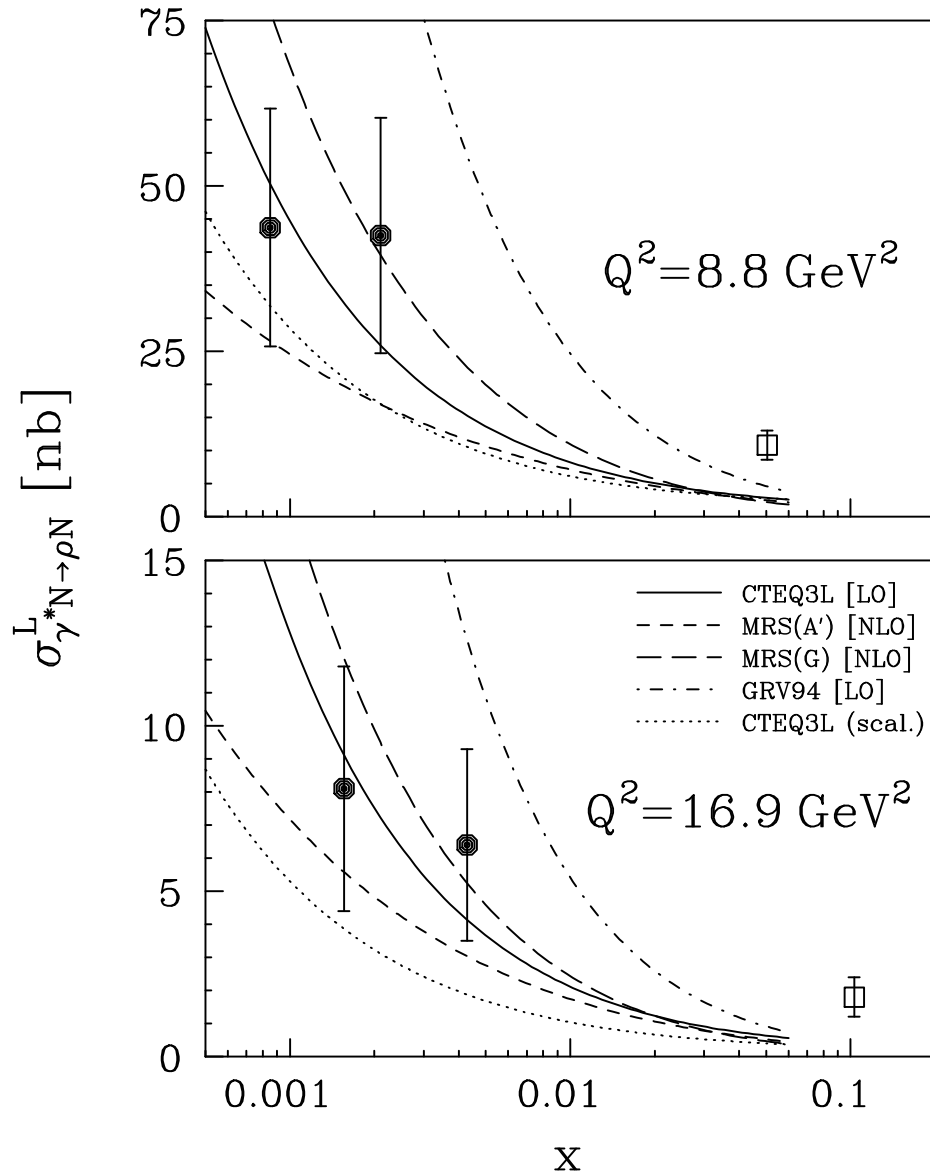


FIG. 10. The total longitudinal cross section, $\sigma_{\gamma^* N \rightarrow \rho N}^L$, calculated from Eq. (12) for several recent parametrizations of the gluon density in comparison with experimental data from ZEUS [6] (full circles) and NMC [32] (squares).

We discussed in Sect. IV.C that next-to-leading order corrections should lead to a decrease of the scale effective in the gluon densities, i.e., the virtualities that enter in the argument of $\alpha_s(Q^2)G_N(x, Q^2)$, due to the fact that $b_{\gamma_L^* \rightarrow \rho}(Q^2)$ is substantially larger than $b_{\sigma_L}(Q^2)$. This results in a decrease of the ρ production cross section as illustrated in Fig. 10 for the CTEQ3L parametrization through the dotted lines.

One can see from the figure that we substantially underestimate the cross section at lower energies which, in turn, correspond to rather large x : for example $\langle x \rangle = 0.103$ for the NMC point at $Q^2 = 16.9 \text{ GeV}^2$. This kinematics is well beyond the x -range specified in Eq. (8), and the frozen approximation, which we use, is inapplicable. Qualitatively, one can expect that, in this situation, quantum diffusion of the $q\bar{q}$ pair would lead to an increase of its interaction cross section, and hence to agreement with the observed cross section.

C. Absolute magnitude of the J/Ψ photoproduction cross section

In a recent work by Ryskin et al. [38], J/Ψ photoproduction data were compared with the corresponding pQCD predictions. For the latter, the nonrelativistic constituent quark model for the J/Ψ 's wave function was employed, and Fermi motion and $M_{J/\Psi} \neq 2m_c$ corrections were estimated to leave the cross section unaltered. On the other hand, we argued in Sect. IV.B that there is a strong reduction (~ 0.13) of the naive pQCD prediction for J/Ψ photoproduction due to those presymptotic effects. Here, we thus compare our predictions with the data, while either accounting for the presymptotic corrections, i.e. the factor $T_V(Q^2)$ of Eq. (23) and the $M_{J/\Psi} \neq 2m_c$ correction of Eq. (25), or while leaving them out.

Setting, $\eta_V = 2$ and $Q^2 \rightarrow \bar{Q}^2 = \frac{Q^2 + 4m_c^2}{4}$ as suggested in Ref. [38], our Eq. (12) yields

$$\left. \frac{d\sigma_{\gamma^{(*)}N \rightarrow J/\Psi N}^L}{dt} \right|_{t=0} = \frac{\pi^3 \Gamma_{J/\Psi \rightarrow e^+e^-} M_{J/\Psi} \alpha_s^2(\bar{Q}) T_V(Q^2)}{12 \alpha_{EM} \bar{Q}^6} \left| \left(1 + i \frac{\pi}{2} \frac{d}{d \ln x} \right) x G_N(x, \bar{Q}) \right|^2, \quad (30)$$

which agrees with the result given in [5,38] if we neglect the Fermi motion and $M_{J/\Psi} \neq 2m_c$ corrections, i.e., if we set $T_V(Q^2)$ of Eq. (23) to 1 and replace m_c by $M_{J/\Psi}/2$. On the

other hand, we can also use the results of our analysis on the relevant transverse distances of Sect. III.A (see Fig. 4) to estimate the scale, \bar{Q} , effective in $\alpha_s(\bar{Q})xG_N(x, \bar{Q})$ in Eq. (30). As outlined in Sect. IV.C, we find for J/Ψ photoproduction $\bar{Q}^2 \approx 5.1 \text{ GeV}^2$ which is substantially higher than the estimate of Ref. [38] – $\bar{Q}^2 = 2.4 \text{ GeV}^2$ – and which leads to an increase of the respective cross sections by a factor of about 1.5 for the logarithmic potential of Ref. [30]. Taking the experimental value for the slope parameter of $B_{J/\Psi} \approx 4.5 \text{ GeV}^{-2}$, the cross section for diffractive J/Ψ photoproduction is calculated from Eq. (30), and corresponding results are shown in Fig. 11 for various recent parametrizations of the gluon density.

Thus, if Fermi motion, the $m_c \neq M_{J/\Psi}/2$ correction and Q^2 rescaling are accounted for, the predictions of the pQCD model and the photoproduction data agree, at large W , within the uncertainties in the existing gluon distributions for the logarithmic potential model [30], which gives a smaller suppression as it has a m_c close to the current quark mass (cf. discussion in Sect. IV.B).

It is instructive, also, to consider the ratio of the J/Ψ photoproduction and the longitudinal ρ -meson electroproduction cross sections, $\sigma(\gamma p \rightarrow J/\Psi p)/\sigma(\gamma_L^* p \rightarrow \rho p)$, for $Q^2 = 8.8 \text{ GeV}^2$ and at the same x . We find that the various gluon distributions lead to very similar ratios since the gluon densities enter at about the same virtualities. In detail, we find $\sigma(\gamma p \rightarrow J/\Psi p)/\sigma(\gamma_L^* p \rightarrow \rho p)|_{theo} \approx 0.9$ with the \bar{Q} rescaling and 0.6 without both at $x = 2.1 \cdot 10^{-3}$ and $x = 8.5 \cdot 10^{-4}$ with a theoretical error $\approx \pm 0.4$ due to uncertainties of the estimate of the suppression factor $T_V(Q^2)$. The experimental data yield 1.2 ± 0.6 at $x = 2.1 \cdot 10^{-3}$ and 1.6 ± 0.7 at $x = 8.5 \cdot 10^{-4}$, and thus the theoretical prediction for this ratio is no more than 1σ below the value we extract from the data.

Note, also, that, in a truly relativistic description, for photoproduction – where only transversely polarized photons contribute – the suppression factor of Eq. (23) would contain an extra factor $\propto \frac{1}{4z(1-z)}$, which, in turn, would reduce the suppression by about 20%. At the same time, the analysis of the essential interquark distances (in Sect. III.A) seems to indicate that the coupling of the two gluons to the charmonium meson is more

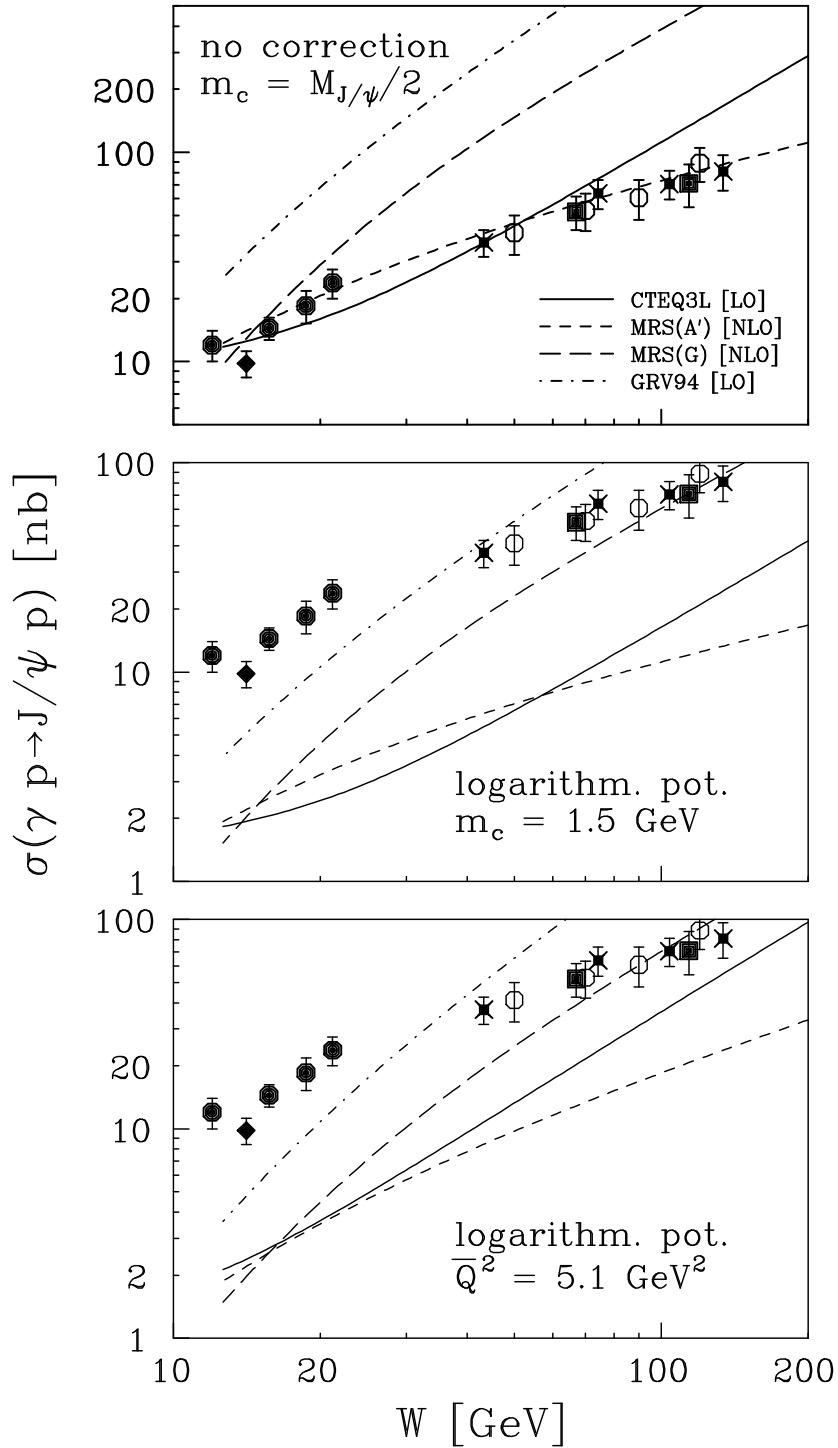


FIG. 11. The diffractive J/Ψ photoproduction cross section compared with experimental data from E401 [10] (full circles), E516 [11] (diamonds), ZEUS '93 [8] (squares), and preliminary ZEUS '94 (circles) and H1 (stars) data [12]. (a): no corrections ($\bar{Q} = M_{J/\Psi}/2$), (b): with the corrections of Sect. IV.B ($\bar{Q} = m_c$) (c): ditto (but with Q^2 rescaling: $\alpha_s x G_N$ evaluated at \bar{Q} based on $b_{J/\Psi}$).

complicated than assumed in the nonrelativistic description. In particular, the interaction of the exchanged gluons with the interquark potential is not suppressed. Only in the approximation where the mass of c quark tends to infinity, this effect would be small ($\sim \frac{l_t^2}{(m_c \alpha_s)^2}$) where l_t is the transverse momentum of the exchanged gluon.

One should also notice that in the fixed target experiments [10,11], the recoil proton was not detected and the corresponding cross sections could thus have been overestimated. Also, it was demonstrated by Jung et al. [39] that, in the kinematics of these experiments, the photon-gluon fusion mechanism could yield up to 50% of the cross section. Besides, the coherence condition of Eq. (8) is violated for J/Ψ photoproduction for $W \leq 12$ GeV.

Also, the qualitative agreement of our predictions for the J/Ψ photoproduction cross section with the data hints that the same approach could be used to calculate the total J/Ψ -N interaction cross section. The inspection of Fig. 3 – at $b \approx 0.40$ fm – shows that such a model approach predicts a rather fast increase of this cross section with energy (in this case $x = M_{J/\Psi}^2/s$) which may appear important for the interpretation of AA collisions. Note that the transverse distances relevant for J/Ψ scattering are larger than those for J/Ψ photoproduction where small b 's are enhanced due to the presence of the photon's wave function in the integral.

D. Q^2 dependence of ρ -meson electroproduction

Let us now analyze the predictions of Eq. (12) for the Q^2 dependence of the vector meson yield. One may conclude from inspection of this equation that it leads to a $1/Q^6$ dependence of the cross section. There are, however, two QCD effects which substantially modify this naive expectation. At large Q^2 , where higher order corrections can be neglected, Eq. (12) predicts a Q^2 dependence of the cross section which is substantially slower than $1/Q^6$ because the gluon densities fastly increase with Q^2 at small x . Numerically, the factor $(\alpha_s(Q) xG_N(x, Q))^2$ in Eq. (12) is $\propto Q^n$ with $n \sim 1$. To illustrate this point, we define the effective power of the Q^2 dependence of $[\alpha_s(Q) xG_N(x, Q)]^2$ as

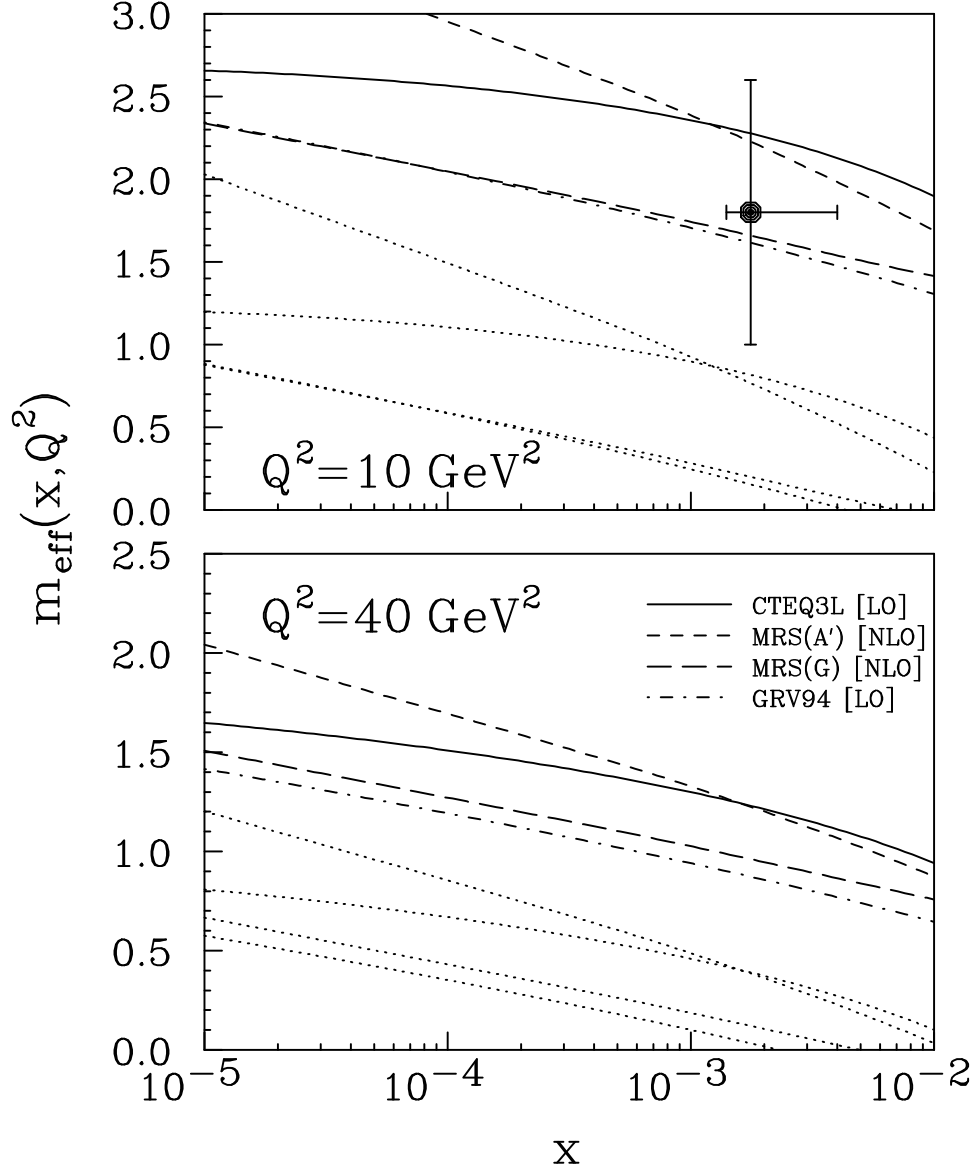


FIG. 12. Effective power of the Q^2 dependence of $(\alpha_s(Q) x G_N(x, Q))^2$ as defined in Eq. (31) (dotted lines) and including preasymptotic effects from quark Fermi motion together with the ZEUS data point [6].

$$m_{eff}(x, Q^2) \equiv 2 \frac{\partial \ln (\alpha_s(Q)xG_N(x, Q))}{\partial \ln Q} . \quad (31)$$

Results for $m_{eff}(x, Q^2)$ using several current parametrizations of the gluon distributions in the nucleon [42,43,27] are presented in Fig. 12 for $Q^2=10$ and 40 GeV^2 as functions of x (dotted lines) together with the experimental ZEUS data point [6]. One can see that, typically, they reduce the Q^2 dependence by one power of Q for $Q^2 \sim 10 \text{ GeV}^2$.

A *preasymptotic* effect may come from higher order corrections to the $1/Q^6$ factor, see, for instance, the discussion in Sect. IV. The corresponding term, $T(Q^2)$ of Eq. (21) and depicted in Fig. 5, yields an effective power of $p_{eff}(Q^2) = \frac{\partial \ln T(Q^2)}{\partial \ln Q}$ to the Q^2 dependence of the cross section, where $p_{eff}(10\text{GeV}^2) \approx 1.5$ and $p_{eff}(40\text{GeV}^2) \approx 0.8$. Thus, combined, these two effects result in

$$n_{eff}(x, Q^2) = 6 - \left(m_{eff}(x, Q^2) + p_{eff}(Q^2) \right) , \quad (32)$$

as shown also in Fig. 12. One can see from the figure that, in the ZEUS range, the n_{eff} we find is consistent with the experimental number of ZEUS. Note that if we include Q^2 rescaling, which was discussed in Sect. IV.C, the n_{eff} 's we find increase by about 0.3 for the kinematics of the HERA experiment.

VI. RESTORATION OF FLAVOR SYMMETRY

Longitudinal vector meson production is dominated by small interquark distances in the vector meson wave function. Therefore the factorization/decoupling theorem can be used to calculate the cross section for hard diffractive processes in QCD without any model assumptions. For $M_V^2 \ll Q^2$, all dependence on the quark masses and thus on flavor is contained in the light-cone wave function of the vector meson and not in the scattering amplitude. This prediction is non-trivial, since experimentally the coherent photoproduction of mesons containing strange or charm quarks is strongly suppressed as compared to the SU(4) prediction for the ratio of the production cross sections for various vector mesons, which is

$$\rho^o : \omega : \phi : J/\Psi = 9 : 1 : 2 : 8 . \quad (33)$$

Experimentally, this suppression factor is ≈ 4 for ϕ -mesons and ≈ 25 for the J/Ψ . Thus, QCD predicts a dramatic increase of the $\phi : \rho^o$ and $J/\Psi : \rho^o$ ratios at large Q^2 [9]. We expect that for the $\phi : \rho$ -ratio, the pQCD limit would be reached rather early, while the restoration of $SU(4)$ in J/Ψ -meson production would require extremely high Q^2 . This will be clarified further in the next section. Besides, QCD predicts a slow increase of the relative yield of heavy flavor production with decreasing x since the virtuality which enters in the gluon distribution is larger for heavy flavor production.

Moreover, an additional enhancement of heavy flavor production is expected since, for heavy quarkonium states, the probability for a q and \bar{q} to be close together is larger. In fact, Eq. (12), which was derived from QCD, predicts for the production ratio of mesons V_1 and V_2 , at large Q^2 , that

$$\left. \frac{\sigma(\gamma_L^* + T \rightarrow V_1 + T)}{\sigma(\gamma_L^* + T \rightarrow V_2 + T)} \right|_{Q^2 \gg M_{V_1}^2, M_{V_2}^2} = \frac{M_{V_1} \Gamma_{V_1 \rightarrow e^+ e^-} \eta_{V_1}^2(Q^2)}{M_{V_2} \Gamma_{V_2 \rightarrow e^+ e^-} \eta_{V_2}^2(Q^2)} . \quad (34)$$

Values of η_V for mesons built of light quarks seem to be close to the asymptotic value of $\eta_V = 3$ already for moderate $Q^2 \sim 10 \text{ GeV}^2$. This reflects the observation of a QCD sum rule analysis [31] as well as lattice QCD [44] and the instanton liquid model [45] that the nonperturbative interaction in the vector channel is weak.

Based on the measured values of $\Gamma_{V \rightarrow e^+ e^-}$ and estimates of η_V [31] for ρ and ϕ and the charmonium model for J/Ψ , we observe that Eq. (12) predicts a significant enhancement of ϕ and J/Ψ production as compared to the $SU(4)$ prediction of Eq. (33):

$$\rho^o : \omega : \phi : J/\Psi = 9 : (1 * 0.8) : (2 * 1.0) : (8 * 1.9) , \quad (35)$$

At very large $Q^2 \gg M_V^2$, the $q\bar{q}$ wave functions of all mesons should converge to a universal asymptotic wave function with $\eta_V = 3$ [31]. In this limit, further enhancement of heavy resonance production is expected,

$$\rho^o : \omega : \phi : J/\Psi = 9 : (1 * 0.8) : (2 * 1.2) : (8 * 3.5) . \quad (36)$$

It is important to investigate these ratios separately for the production of longitudinally polarized vector mesons, where hard physics dominates, and for transversely polarized vector mesons, where the interplay between soft and hard physics is most important.

VII. PRODUCTION OF EXCITED VECTOR MESON STATES

Equation (12) is applicable also to the production of excited vector meson states if their masses $M_{V'}$ satisfy the condition that $M_{V'}^2 \ll Q^2$. In this limit, it predicts comparable production of excited and ground states. There are no estimates of $\eta_{V'}$; so, following the above discussion, we assume that the $q\bar{q}$ wave functions of a ρ' , ω' and ϕ' are close to the asymptotic value, and, as a rough estimate, we will assume that $\eta_{V'} = \eta_V$. Using the information on the mesons' decay widths from the Review of Particle Properties [46] and results of an analysis by Clegg and Donnachie [47] of the properties of excited light vector mesons, we find that:

$$\begin{aligned}
\rho(1450) : \rho^o &\approx 0.45 - 0.95 , \\
\omega(1420) : \omega &\approx 0.46 , \\
\rho(1700) : \rho^o &\approx 0.22 \pm 0.05 , \\
\omega(1600) : \omega &\approx 0.48 , \\
\phi(1680) : \phi &\approx 0.85 , \\
\Psi' : J/\Psi &\approx 0.5 .
\end{aligned}
\tag{37}$$

In view of substantial uncertainties in the experimental widths of most of the excited states as well as in the values of $\eta_{V'}$, these numbers can be considered as good to about a factor of two (except for the Ψ' where Γ_V is well known). For example, if we would just sum over the partial widths of the $\omega(1600)$, as listed in the Review of Particle Properties [46], we would get $\omega(1600) : \omega \geq 0.93$. Note, also, that in quark models one would expect $\rho(1450) : \rho \approx \omega(1420) : \omega$ and $\rho(1700) : \rho \approx \omega(1600) : \omega$, which is not satisfied in the cases of the $\rho(1700)$ and $\omega(1600)$.

Note that the essential transverse momenta in the $q\bar{q}$ wave function of the excited states are likely to be significantly larger than in the ground state. This is dictated by the spectrality condition in the bound state equation for the minimal Fock $q\bar{q}$ component of the light-cone wave function of the vector meson, which ensures that

$$\frac{m^2 + k_t^2}{z(1-z)} \geq M_V^2. \quad (38)$$

The estimate which follows from this equation, $\sqrt{\langle k_t^2 \rangle} \approx M_{V'}/2$, shows that the transverse momenta characteristic for the minimal Fock component of the wave function should increase with the mass of the excited state. Hence, we made a model estimate for the Q^2 dependence of the ratio $\rho(1700) : \rho$ taking model I type wave functions for the k_t -dependence ($\phi(k_t) \propto \frac{1}{(k_t^2 + \lambda^2)^2}$ as introduced in Sect. III) with $\sqrt{\langle k_t^2(\rho) \rangle} = 450 \text{ MeV}/c$, and $\sqrt{\langle k_t^2(\rho) \rangle} / \sqrt{\langle k_t^2(\rho') \rangle} = M_\rho / M_{\rho'}$. The corresponding results for the Q^2 dependence of the ratio $\rho(1700) : \rho$ are displayed in Fig. 13 as a solid line. We also present in this figure the ratios for $\Psi' : J/\Psi$ and $J/\Psi : \rho$ production, normalized to their asymptotic values at $Q^2 \rightarrow \infty$ given in Eqs. (36) and (37).

Larger average momenta in the excited mesons' wave functions imply that the important virtualities in the gluon density essential for a given Q^2 are larger for the production of excited states. This should manifest itself also in an increase of the ratios $V' : V$ with decreasing x , since the parton distributions depend on $\langle k_t^2(V) \rangle$, and they increase faster at larger $\langle k_t^2(V) \rangle$.

For those excited states, which in the nonrelativistic quark model are just radial excitations of the corresponding ground state (presumably the $\rho(1450)$ and the $\omega(1420)$), and in the Q^2 region where one can apply perturbative QCD, our predictions for the increase of the $V' : V$ ratios are qualitatively similar to those of Nemchik et al. [14], who predict an increase of $\rho' : \rho$ to 1 at large Q^2 . At the same time, in the calculations of Ref. [14], the effects of the quark Fermi motion in the diffractively produced vector mesons, which constitute the dominant contribution to the production ratios at larger Q^2 , were not accounted for. As a result, the saturation of the $V' : V$ ratio occurs in the model of, e.g., Ref. [14] already at $Q^2 \sim 10 \text{ GeV}^2$.

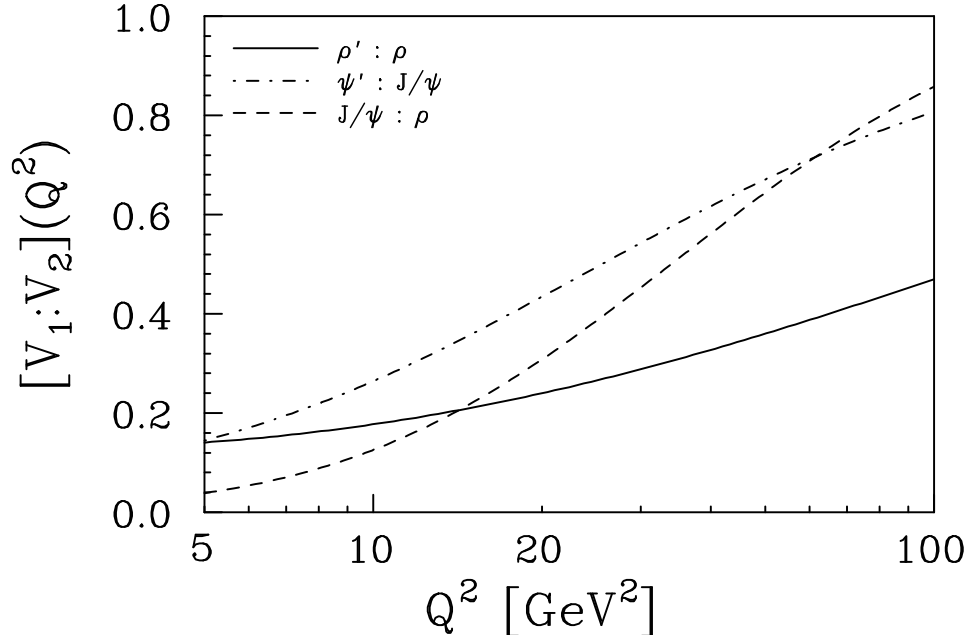


FIG. 13. Relative yields in the diffractive electroproduction of various vector mesons normalized to their asymptotic values at $Q^2 \rightarrow \infty$ given in Eqs. (36) and (37).

Another important difference stemming from the use of nonrelativistic oscillator wave functions, which do not take into account the Q^2 evolution of the minimal Fock space wave functions (which is a strict consequence of QCD [19]), is the qualitative difference between the behavior of radial and orbital (e.g. D -state) excitations. The production of the latter is strongly suppressed at large Q^2 in the approximation considered in Refs. [13,14,17], while we find essentially the same rate for both classes of excited states. So without mentioning this explicitly, the authors of Refs. [13,14,17] considered ρ' and ϕ' corresponding to radial excitations only.⁹ According to the current interpretation of the data, the $\rho(1450)$ and $\omega(1420)$ are radial excitations, while the $\rho(1700)$ and $\omega(1600)$ are D -wave states. Note that for the cases where the uncertainties in the analysis of Clegg and Donnachie [47] for $\Gamma_{V \rightarrow e^+e^-}$ are smaller - $\omega(1420)$ and $\omega(1600)$ - we find that the expected yields at large Q^2 as given by Eq. (37) are comparable.

⁹We are indebted to B.Z. Kopeliovich for clarifying what ρ' -state they considered.

To summarize, a substantial production of excited resonance states is expected at large Q^2 at HERA. A measurement of these reactions may help to better understand the dynamics of the diffractive production of vector mesons as well as the light-cone minimal Fock state wave functions of these excited states. It may provide the first *three dimensional* images of these states, and it would also allow to look for the second missing excited ϕ state, which is likely to have a mass of about 1900 MeV to follow the pattern of the ρ , ω and J/Ψ families.

The relative yield of excited states produced by virtual photons is expected to be higher than that for real photons since the Vector Dominance Model (VDM) [41] together with Eq. (12) leads to

$$\begin{aligned} \frac{\sigma(\gamma + N \rightarrow V + N)}{\sigma(\gamma + N \rightarrow V' + N)} \frac{\sigma(\gamma_L^* + N \rightarrow V' + N)}{\sigma(\gamma_L^* + N \rightarrow V + N)} \Big|_{Q^2 \gg M_{V'}^2, M_V^2} &= \\ &= \frac{M_{V'}^2}{M_V^2} \frac{\eta_{V'}^2(Q^2)}{\eta_V^2(Q^2)} \geq \frac{M_{V'}^2}{M_V^2}. \end{aligned} \quad (39)$$

In the last step, we used the empirical observation that for the effective cross sections of $V'N$ and VN interactions, which enter in the VDM model,¹⁰ $\frac{\sigma_{tot}(V'N)}{\sigma_{tot}(VN)} \leq 1$, and that

¹⁰Note that these effective cross sections have no direct relation to the genuine interaction cross sections. For example, based on geometrical scaling, one expects the interaction cross section to increase with the size of the projectile approximately as $R = \sigma_{tot}(\Psi'N)/\sigma_{tot}(J/\Psi N) \sim R_{\Psi'}^2/R_{J/\Psi}^2 \sim 4$. However, if one applies the VDM to the extraction of cross sections from photoproduction of J/Ψ and Ψ' , one finds $R \sim 0.7 \sim M_{J/\Psi}^2/M_{\Psi'}^2$. This trend seems to reflect effects of color screening in the production of heavy quarkonium states [48,1]. Note, also, that photoproduction data do not resolve the $\rho(1430)$ and $\rho(1700)$. In the case of ρ' photoproduction off nuclei, similar nuclear absorption effects are observed for the production of the ρ and ρ' , indicating $\sigma(\rho'N) \approx \sigma(\rho N)$. At the same time, application of the VDM to the process $\gamma p \rightarrow \rho' p$ leads to $\sigma(\rho'N) \approx (0.37 \pm 0.07) \sigma(\rho N)$, where we used the analysis of Ref. [47] of the $V \rightarrow e^+e^-$ widths and the data of Chapin et al. [49] for diffractive ρ' production. The observed

η_V and $\eta_{V'}$ are close to their asymptotic values for light mesons while for heavy quark systems the values of η'_V should be closer to the static limit of $\eta_V = 2$.

Equation (12) is applicable also to vector meson production in weak processes. Consider, for example, the diffractive production of a $D_s^{*\pm} = (c\bar{s})$ meson in $W^\pm N$ scattering. To calculate this cross section, it is sufficient to substitute in Eq. (12) the electromagnetic coupling constant with $g \cos \theta_C$, where θ_C is the Cabibbo angle.

It is often discussed that the production of hadrons in e^+e^- annihilation at intermediate masses ($M_h \leq 2 \div 2.5$ GeV) can be described as the production and decay of several vector meson resonances. Within this approximation, we can generalize Eq. (12) to the case of diffractive electroproduction of hadron states in the continuum. To deduce the relevant formulae, we assume that for excited vector meson resonances η_V is close to its asymptotic value, $\eta_V = 3$. This assumption really follows from the application of the dispersion sum rule approach. In the limits $M_h^2 \leq 5\text{GeV}^2 \ll Q^2$, $x \ll 1$ and $Q^2 \rightarrow \infty$, we obtain:

$$\left. \frac{d\sigma_{\gamma^* N \rightarrow hN}^L}{dt dM^2} \right|_{t=0} = \frac{9T^2(Q^2)M_h^2 \sigma(e^+e^- \rightarrow h) \alpha_s^2(Q) \left| \left(1 + i\frac{\pi}{2} \frac{d}{d \ln x}\right) x G_T(x, Q) \right|^2}{4N_c^2 \alpha_{EM} Q^6}. \quad (40)$$

It is worth emphasizing that in the case of diffraction to high enough masses, where the intermediate γ^* state can be approximated by a free $q\bar{q}$ pair, the contribution of large transverse distances is not suppressed and the cross section gets both soft and hard contributions. Consequently, in the intermediate M_h^2 range, where resonances are still present but the continuum is already essential, one should expect a faster increase with energy (at fixed Q^2) of the resonance contribution.

pattern indicates that the production of ρ' is dominated by average quark-gluon configurations (large absorption cross section), while the probability of these transitions is suppressed since the transition $\gamma^* \rightarrow V$ emphasizes the role of small configurations. Another possible interpretation (which maybe complementary to the one above) is a large contribution of nondiagonal transitions $\rho' \rightarrow \rho$ in the scattering off nuclei. CT arguments [50] (p.170) suggest that $V \rightarrow V'$ transitions could indeed be very appreciable.

To summarize, the investigation of exclusive diffractive processes appears to be the most effective method to measure the minimal Fock state $q\bar{q}$ component of the wave functions of vector mesons as well as the light-cone wave functions of any small mass hadron system having angular momentum one. It seems that the cross sections of these processes are rather sensitive to the three dimensional distribution of color within the wave functions of vector mesons. This observation could be very helpful in expanding methods of lattice QCD into the domain of high energy processes.

VIII. THE KINEMATICAL BOUNDARY FOR THE REGION OF APPLICABILITY OF THE LEADING LOGARITHM APPROXIMATIONS TO QCD

In the above, we have explained that the increase of the cross section with energy ($\frac{1}{x}$) at fixed Q^2 originates from the energy dependence of the $q\bar{q}T$ cross section, see Eq. (7) and Fig. 3. But, in the region dominated by hard physics, the value of this cross section is restricted by the unitarity of the S -matrix, and even more stringent restrictions follow from the condition that the leading twist term should be significantly larger than the next to leading twist term. In detail, let us consider the scattering of a small object, a $q\bar{q}$ pair, from a large object, a nucleon. If only hard physics were relevant for the increase of the parton distributions at small x , the radius of the $q\bar{q}$ -nucleon interaction should be practically independent on energy, because, in this case, Gribov diffusion in the impact parameter space would be determined by the scale characteristic for hard processes. We shall explore this observation to establish the region of applicability of the leading $\ln \frac{1}{x}$ and $\ln \frac{Q^2}{\Lambda_{QCD}^2}$ approximations.

Thus, the geometrical restriction is that, in the hard regime, the inelastic cross section cannot exceed the geometrical size of the target nucleon. An equivalent, but practically more convenient, formulation of this important property of hard processes is that the slope of the differential cross section should not increase with energy. It is just this property of hard processes which gives the possibility to deduce an unitarity limit for their cross

sections and/or on the region dominated by hard physics.

We will start our considerations with the derivation of the boundary for the region where the decomposition over powers of $\frac{1}{Q^2}$ can be a sensible approximation. A formal method to deduce this restriction is to consider scattering of heavy quarkonium $Q\bar{Q}$ states from a hadron target, and to vary the mass of the heavy quark. Since the result of such a derivation is evident, in this paper we use an equivalent but shorter way to deduce this inequality [9]: We establish the limit by applying the optical theorem to calculate the elastic cross section for scattering of a small-transverse-size $q\bar{q}$ pair off a nucleon:

$$\frac{d\sigma_{el}}{dt}(q\bar{q}N) = \frac{\sigma_{tot}^2}{16\pi} e^{Bt} (1 + \beta^2) , \quad (41)$$

where

$$\beta = ReA_{q\bar{q}N}/ImA_{q\bar{q}N} \simeq \frac{\pi}{2} \frac{d \ln(xG_N(x, Q^2))}{d \ln x} . \quad (42)$$

For simplicity, we parametrize the dependence of the differential cross section on the momentum transfer t , at small t (which dominate the cross section), in the form of an exponential. As the observed t dependence of hard diffractive processes is close to that given by the square of the nucleon's electromagnetic form factor, i.e., $\sim \exp(\frac{r_N^2}{3}t)$, to visualize the deduced limit, it is convenient to express the experimental value of the slope of the t dependence of the cross section through the average quadratic radius of a nucleon: $B \approx 4 \div 5 \text{ GeV}^{-2} \approx \frac{r_N^2}{4}$ where $r_N = 0.8 \text{ fm}$. It follows from QCD (cf. discussion in Sect. III.A) that this value should be universal for all hard processes. Existing data on hard diffractive production of vector mesons are in line with this QCD prediction, and we can use it to calculate the elastic cross section:

$$\sigma_{el} = \frac{\sigma_{tot}^2}{16\pi B} (1 + \beta^2) \approx \frac{\sigma_{tot}^2}{4\pi r_N^2} (1 + \beta^2) . \quad (43)$$

In the derivation of the boundary for the region where the leading $\ln \frac{1}{x}$ and $\ln \frac{Q^2}{\Lambda_{QCD}^2}$ approximations are applicable, one should actually add to Eq. (43) the contribution from proton dissociation, i.e., one should multiply σ_{el} by $(1 + \gamma)$ where $\gamma \sim 10 \div 30\%$.

The necessary condition for the applicability of the decomposition of the deep inelastic cross section over powers of Q^2 is that the leading twist contribution should exceed non-leading twist terms. In our case, this implies that $\sigma_{inel} \gg \sigma_{el}(1 + \gamma)$, where γ accounts for the dissociation of the proton. So, the boundary for the applicability of the decomposition over powers of $1/Q^2$ is $\frac{\sigma_{el}(1+\gamma)}{\sigma_{inel}} = y \ll 1$. Using Eq. (43) and above discussed value of B , we obtain:

$$\sigma_{inel} \ll \frac{\pi r_N^2}{(1 + \beta^2)} \frac{4y}{(1 + \gamma)(1 + y)^2} . \quad (44)$$

Thus the region of applicability of the QCD evolution equation is:

$$\sigma_{inel}(q\bar{q}N) = \frac{\pi^2}{3} b^2 \alpha_s \left(\frac{9.2}{b^2} \right) xG_p \left(x, \frac{9.2}{b^2} \right) \ll \frac{\pi r_N^2}{(1 + \beta^2)} \frac{4y}{(1 + \gamma)(1 + y)^2} \quad (45)$$

The unitarity of the S -matrix, which corresponds to the condition $y = 1$, was discussed in Refs. [51,52,9]. It can only be translated into an actual kinematical boundary if one considers purely hard physics, where B is restricted by the nucleon size. In general, however, the slope B and its energy dependence have to be evaluated separately, which has not been done so far. Such analysis would lead to the Froissart limit, with B and the cross section slowly increasing with energy. Note also that Eq. (7) has been deduced in the approximation where only the leading power of b^2 has been taken into account. A more stringent limit follows from the requirement that the single particle density in the center of rapidity should be positive. Really, it follows from the application of Abramovskii, Gribov and Kancheli (AGK) combinatorics [53] that this multiplicity is proportional to $\sigma_{inel} - 4(\sigma_{el} + \sigma_{diff})$. Thus, in the approximation when only one hard rescattering is accounted for, we have $y \leq 1/4$.

Therefore, the kinematical boundary for the region of applicability of the leading logarithm approximation is significantly more stringent than that given by the unitarity condition:

$$\sigma_{inel}(q\bar{q}N) = \frac{\pi^2}{3} b^2 \alpha_s \left(\frac{9.2}{b^2} \right) xG_p \left(x, \frac{9.2}{b^2} \right) \ll \frac{16}{25} \frac{\pi r_N^2}{(1 + \beta^2)(1 + \gamma)} \quad (46)$$

Eq. (46) allows us to estimate down to what $x \equiv x_{lim}$. the equations for σ_L and $\sigma_{\gamma_L^* N \rightarrow \rho N}$ can be applied. For certainty, we choose $\gamma = 0.2$ in our evaluation. Results of a calculation

of $x_{lim.}(Q^2)$ based on Eq. (46) for the two most current gluon parametrizations are presented in Fig. 14. The boundary is even more stringent for ρ -meson production since the average $b(Q)$ are larger in this case (see the dashed and dotted curves in Fig. 14). Actually, it is likely that the slow down starts earlier, in particular due to dispersion in b . However, a detailed analysis of this effect is beyond the scope of this work.

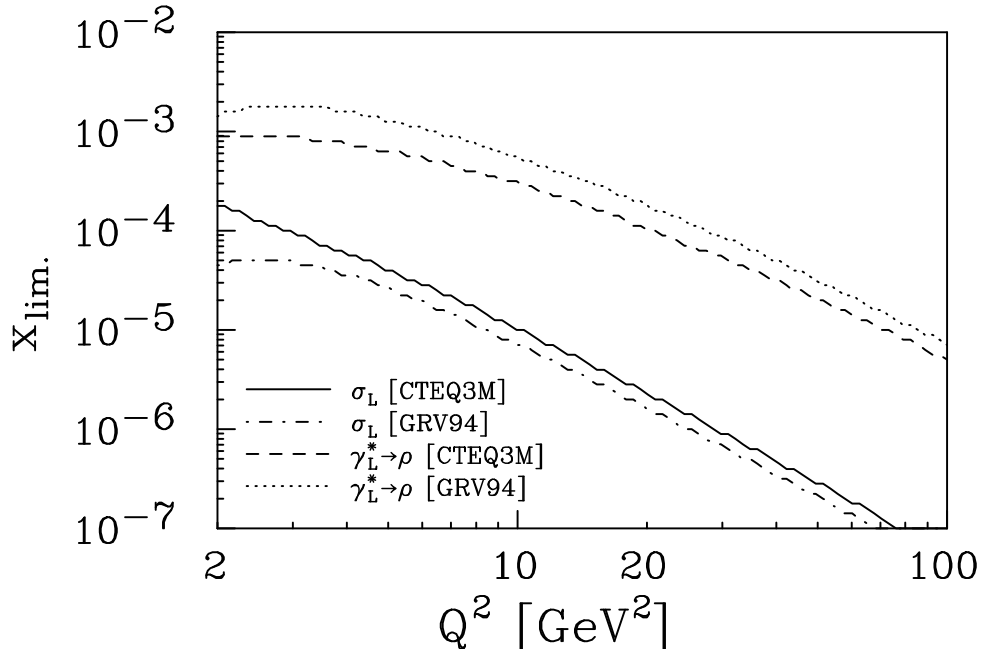


FIG. 14. The boundary of the region of applicability of pQCD for a nucleon target, $x_{lim.}(Q)$, as determined from Eq. (46) for deep inelastic scattering (σ_L) as well as diffractive electroproduction of ρ -mesons ($\gamma_L^* N \rightarrow \rho N$).

The advantage of the approach used in this paper, as compared to previous attempts (for a review and references see Refs. [54,55]), is that we actually deduce the QCD formulae for the cross section for scattering of a $q\bar{q}$ pair off a hadron target. For this cross section, the geometrical limit (including numerical coefficients) unambiguously follows from the unitarity of the S -matrix, that is from the geometry of the collision (under the assumptions made in Refs. [54,55] on the dominance of hard physics near the unitarity limit). As a result, we obtain a more stringent inequality which contains no free parameters. Recently, a quantitative estimate of the saturation limit was obtained [56] by considering

the GLR model [57,58] of nonlinear effects in the parton evolution and requiring that the nonlinear term should be smaller than the linear term. The constraint obtained in that paper is numerically much less restrictive than our result: the parameter characterizing the scale of corrections found in Ref. [56] differs from ours by a numerical factor $\sim \frac{1}{16}$. The qualitative reason for this difference is that the GLR model neglects elastic rescatterings of the $q\bar{q}$ pair, and it does not take into account the requirement of positiveness of the single particle density. The consideration of a specific cut of the double scattering diagram, which corresponds to the shadowing of the single hadron multiplicity, and the requirement that the single multiplicity should be positive leads, within this model, to the restriction that $\sigma_{el} + \sigma_{diff}$ cannot exceed $1/4 \sigma_{inel}$. The numerical coefficient follows then from the application of Abramovskii, Gribov and Kancheli (AGK) combinatorics [53]. This observation indicates that, in the GLR model [57,58], hard double scattering may decrease the parton density by not more than 25% (and by no more than the observed diffraction fraction of the cross section which is $\sim 15\%$ at HERA). As usual, if the corrections become large enough, one cannot restrict the consideration to one particular contribution.

We want to point out that the deduced constraint implies only a restriction on the limiting behavior of the cross sections for hard processes, but it gives no clues whether this boundary can be achieved. In reality, the increase of the cross sections of hard processes should slow down already at larger x than those given by the constraint which we deduced here. This is because in the derivation of the boundary we ignore, amongst others, the for Feynman diagrams characteristic diffusion in the parton ladder to large distances, effects related to the dispersion of b as well as other hard diffractive processes which also fastly increase at $x \rightarrow 0$. The dynamical mechanism responsible for the slowing down of the increase of the parton distributions, so that they satisfy, for instance, Eq. (44), is subject of discussions. In particular, the triple Pomeron mechanism for shadowing suggested in Ref. [57] does not lead to large effects at HERA energies, especially if one assumes a homogeneous transverse density of gluons [55,59].

IX. LIMITS OF APPLICABILITY OF THE QCD EVOLUTION EQUATIONS TO THE SCATTERING OFF HEAVY NUCLEI

The application of similar consideration to the scattering off nuclei leads to a more severe restriction on the gluon distribution in nuclei:

$$\sigma_{inel}(q\bar{q}A) \leq \frac{\pi R_A^2}{(1 + \beta^2)} \frac{4y}{(1 + \gamma_A)(1 + y)^2} . \quad (47)$$

Here, R_A is the radius of the nucleus and γ_A stems from the dissociation of the nucleus. $\beta = ReA_{q\bar{q}N}/ImA_{q\bar{q}N}$ is determined from the x dependence of the gluon density and should be universal within a considered approximation. For a heavy nucleus, we may safely substitute $y = 1$ since the total and elastic cross sections are then not far from the black body limit, where $\sigma_{tot}^A \approx 2\pi R_A^2$ and $\sigma_{el}^A \approx \pi R_A^2$, even for moderate values of $\sigma_{inel}(q\bar{q}N)$. In the case of a nuclear target, the limit we consider here is worth a separate investigation since interesting effects may arise in the kinematics where the parton densities of a nucleon are still far from the unitarity limit. A.Mueller and J.Qiu [58] were the first to draw attention to nuclear enhancement of nonlinear effects in the QCD evolution equation.

The inequality of Eq. (47) corresponds to a rather stringent restriction on the gluon distribution in heavy nuclei:

$$\frac{1}{A}xG_A(x, Q^2) \leq \frac{3r_0^2}{\pi\alpha_s A^{1/3}} \frac{Q^2}{9.2} \frac{1}{1 + \beta^2} \frac{4y}{(1 + \gamma_A)(1 + y)^2} , \quad (48)$$

where $R_A = r_0 A^{1/3}$ and $r_0 \approx 1.1$ fm. For $Q^2 = 10$ GeV² $\alpha_s = 0.3$, $\gamma_A = 0$, and $y = 1$, this yields

$$\frac{1}{A}xG_A(x, Q^2 = 10 \text{ GeV}^2) \leq \frac{75}{A^{1/3}} . \quad (49)$$

A more accurate estimate for this constraint could be obtained by using the discussed inequality for each b and then averaging over b but not just taking the value in the mean point.

In the above, to quantify the kinematical bounds for σ_L and vector meson production, we neglected the dispersion over b in the corresponding amplitudes. But, in practice, we

need the amplitude in k_t -space, i.e., the Fourier transform of the cross section which we discussed above with weights given by the wave functions of the photon or vector meson, respectively. For a more accurate estimate, we need to apply the kinematical limit for fixed b and then calculate the cross sections based on Eqs. (13) and (17) with $\sigma_{q\bar{q}T}$ satisfying the bound.

Let us restrict our analysis here to the case of heavy nuclei as targets, where these effects become important at significantly larger x than for a nucleon target, and where uncertainties in the estimate of the region of applicability of the evolution equation are comparatively small. In fact, we will focus our analysis on the region which would be accessible for HERA with nuclear beams and for the LHC: $x \in 10^{-3} \div 10^{-4}$. In this kinematics, the gluon distribution in the nucleon is already known reasonably well from the recent HERA experiments.

To estimate nonlinear effects, we allow $\sigma_{q\bar{q}A}(x, b)$ to reach the unitarity bound, i.e., we set $y = 1$ in Eq. (47), and if $\sigma_{q\bar{q}A}(x, b) \geq \pi R_A^2$, we substitute it by πR_A^2 . Since in the discussed kinematics, the unitarity corrections to $\sigma_{q\bar{q}N}$ are still small, the ratio of cross sections calculated with and without this unitarity correction characterizes the effective gluon shadowing for σ_L and vector meson production. In the case of ρ -meson production, we chose the same wave function as in Sect. III with $\sqrt{\langle k_t^2 \rangle} = 450$ MeV/c. We also checked that varying $\sqrt{\langle k_t^2 \rangle}$ in the range $300 \div 600$ MeV/c practically does not change our results. The relevant ratios, $R_L(A, x, Q^2) = \frac{1}{A} \frac{\sigma_L^* A}{\sigma_L^* N}$ and $R_V(A, x, Q^2) = \frac{1}{A^2} \frac{d\sigma_L^* + A \rightarrow V + A / dt}{d\sigma_L^* + N \rightarrow V + N / dt} \Big|_{t=0}$ are presented in Fig. 15 for $A = 40$ and $A = 238$ and for $Q^2 = 2, 5, 10, 20$ and 40 GeV². For the sake of an easier comparison of the shadowing effects, in the case of ρ -meson production, we present plots for $\sqrt{R_V(A, x, Q^2)}$. Clearly this estimate is an upper bound for these ratios since it neglects absorptive effects for the case when the interaction is not black.

To estimate nuclear shadowing within a dynamical model, we also consider the b -space eikonal approximation for the calculation of the same quantities. We first calculate the total cross section for the $q\bar{q}N$ interaction by means of the optical theorem,

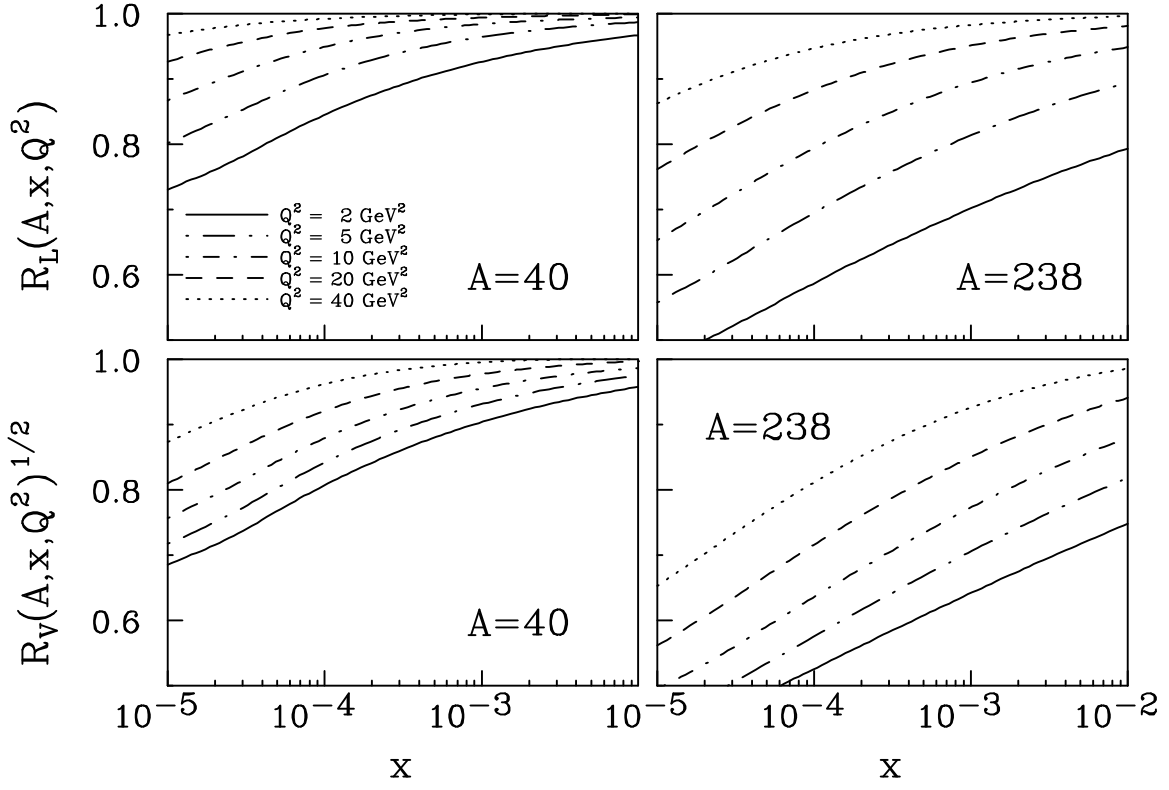


FIG. 15. Nuclear shadowing in DIS in the gluon channel and in diffractive electroproduction of vector mesons is evaluated by employing the nuclear unitarity limit.

$$\sigma_{inel} + \frac{\sigma_{tot}^2}{16\pi B}(1 + \beta^2)(1 + \gamma_A) = \sigma_{tot} , \quad (50)$$

and then evaluate the cross section of the $q\bar{q}A$ interaction for a given impact parameter within the b -space eikonal approximation using the familiar Glauber-Gribov formula [60,61]:

$$R_L(A, x, Q^2) = \frac{1}{A} \frac{Re \left[\int d^2b dz |\psi_{\gamma_L^*}(b, z)|^2 \int d^2B \left(2 - 2e^{-(1-i\beta)\frac{\sigma_{tot}(b)T(B)}{2}} \right) \right]}{\int d^2b dz |\psi_{\gamma_L^*}(b, z)|^2 \sigma_{tot}(b)} , \quad (51)$$

$$R_V(A, x, Q^2) = \frac{1}{A^2} \left| \frac{\int d^2b dz \psi_{\gamma_L^*}(b, z) \psi_{\rho}(b, z) \int d^2B \left(2 - 2e^{-(1-i\beta)\frac{\sigma_{tot}(b)T(B)}{2}} \right)}{\int d^2b dz \psi_{\gamma_L^*}(b, z) \psi_{\rho}(b, z) \sigma_{tot}(b)(1 - i\beta)} \right|^2 , \quad (52)$$

Here, $T(B) = \int_{-\infty}^{+\infty} dz \rho(z, B)$ is the optical thickness of the nucleus and $\rho(z, B)$ is the nuclear density normalized so that $\int_{-\infty}^{+\infty} dz d^2B \rho(z, \vec{B}) = A$. We use Eqs. (51) and (52) to estimate the nuclear shadowing for σ_L and for ρ -meson production employing a realistic nuclear density distribution, $\rho(r) \sim 1/(1 + \exp[(r - R_A)/a])$, where $R_A = 1.1 A^{1/3}$ fm and $a = 0.56$ fm. Corresponding results are presented in Fig. 16.

One can see from Figs. 15 and 16 that significant gluon shadowing is expected at small x , and that shadowing is larger in the ρ -meson channel, i.e., $\sqrt{R_V(A, x, Q^2)} < R_L(A, x, Q^2)$. This is again due to the larger b for ρ -meson production – see the discussion in Sect. III. Also, in line with expectations of the color transparency logic, at fixed large Q^2 , shadowing increases with decreasing x – i.e., $R_L, R_V \ll 1$ for $x \rightarrow 0$ and color transparency *disappears* for small enough x – while, for fixed small x , shadowing decreases with increasing Q^2 – i.e., $R_L, R_V \rightarrow 1$ at large Q^2 and color transparency *appears* for large enough Q^2 .

Furthermore, from Figs. 15 and 16, we observe that the nuclear shadowing which we deduce from the unitarity limit and from the eikonal model is significantly smaller than the black disk limit. This is partly due to the diffuse edge of the nucleus, and a practical conclusion from this observation is that nuclear shadowing of the parton distributions should be considerably larger for central AA collisions where the effects of the nuclear surface should be insignificant.

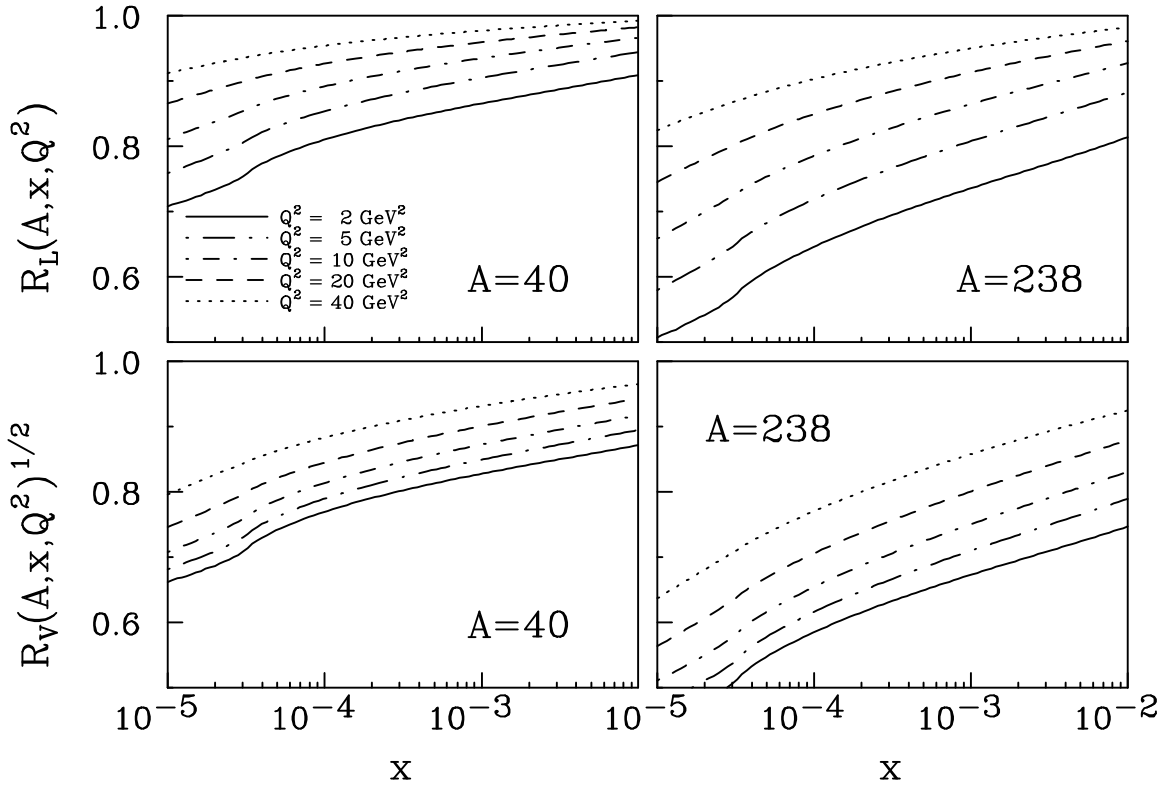


FIG. 16. Nuclear shadowing in DIS in the gluon channel and in diffractive electroproduction of vector mesons is evaluated in b -space eikonal approximation.

Note, however, that even those estimates are still likely to underestimate the relevant shadowing since they do not explicitly include gluon shadowing in the leading twist, i.e. logarithmically decreasing at large Q^2 . Still, our estimate corresponds to significantly larger gluon shadowing than that obtained in a number of previous papers, where it was assumed that for $Q^2 \approx \text{few GeV}^2$ the leading twist shadowing in the gluon channel and for F_{2A} are approximately the same [62,1,63–65]. Note that qualitative arguments in favor of larger shadowing in the gluon channel were presented in Ref. [66]. The quantities R_L and R_V of Eqs. (51) and (52) were also evaluated in Refs. [13,67] using the two-gluon-exchange model, in which the elementary cross section of the interactions with the constituent quarks does not depend on energy. As a result, in this model, attenuation does not depend on x for small x .

In principle, shadowing effects in the kinematics beyond the region of applicability of the evolution equation may change the dependence of the differential cross section on t , the momentum transferred to the nucleus [68]. In that realm, the eikonal approximation leads to the famous pattern with minima and maxima. Another well known feature of the eikonal approximation, which is specific for potentials fastly increasing with energy, is the shrinking of the diffractive peak with energy. Since, within this model, both soft and hard physics are important, the radius of a nucleon may increase with energy, and, for this regime, the unitarity restriction for processes dominated by hard physics, which we discussed above, could be exceeded and the cross section may increase with x , but more slowly as a power of $\ln x$. For a nuclear target, such effects are expected to be insignificant, although for a nucleon target they may be large.

To summarize, the analysis presented in this Section demonstrates that large shadowing effects should be present at small x in the gluon channel. This has a number of implications for high-energy nucleus-nucleus collisions, where the predictions for hadron production strongly depend on gluon shadowing, as was pointed out, for example, in Ref. [69].

ACKNOWLEDGMENTS

We would like to thank H. Abramowicz, J. Bartels, J. Bjorken, S. Brodsky, A. Caldwell, J. Collins, V. Gribov, and A. Mueller for fruitful discussions on the interplay of soft and hard physics and of the methods of their investigation. This work was supported in part by the Israel-USA Binational Science Foundation Grant No. 9200126, by the MINERVA Foundation of the Federal Republic of Germany, and by the U.S. Department of Energy under Contract No. DE-FG02-93ER40771. Two of us (W.K. & M.S.) thank the DOE's Institute for Nuclear Theory at the University of Washington for its hospitality and support during the workshop "Quark and Gluon Structure of Nucleons and Nuclei".

REFERENCES

- [1] L.L. Frankfurt and M. Strikman, Phys. Rep. 160 (1988) 235
- [2] S. J. Brodsky and A. H. Mueller, Phys. Lett. B206 (1988) 685
- [3] L.L. Frankfurt and M. Strikman, Phys. Rev. Lett. 63 (1989) 1914, Erratum ibid. 64 (1990) 815
- [4] S.J. Brodsky, L.L. Frankfurt, J.F. Gunion, A.H. Mueller, and M. Strikman, Phys. Rev. D50 (1994) 3134
- [5] M.G. Ryskin, Z. Phys. C57 (1993) 89
- [6] M. Derrick et al., Preprint DESY-95-133 (1995)
- [7] T. Ahmed et al., Phys. Lett. B338 (1994) 507
- [8] M. Derrick et al., Phys. Lett. B350 (1995) 120
- [9] H. Abramowicz, L.L. Frankfurt, and M. Strikman, Preprint DESY-95-047 (1995)
- [10] M. Binkley et al., Phys. Rev. Lett. 48 (1982) 73
- [11] B.H. Denby et al., Phys. Rev. Lett. 52 (1984) 795
- [12] ZEUS and H1 collaborations: Preliminary '94 data presented at the Durham Workshop on HERA Physics, Sept. 1995, to be published
- [13] B.Z. Kopeliovich, J. Nemchik, N.N. Nikolaev, and B.G. Zakharov, Phys. Lett. B309 (1993) 179
- [14] J. Nemchik, N.N. Nikolaev, and B.G. Zakharov, Phys. Lett. B339 (1994) 194
- [15] J. Nemchik, N.N. Nikolaev, and B.G. Zakharov, Phys. Lett. B341 (1994) 228
- [16] O. Benhar, B.Z. Kopeliovich, C. Mariotti, N.N. Nikolaev, and B.G. Zakharov, Phys. Rev. Lett. 69 (1992) 1156

- [17] O. Benhar, B.G. Zakharov, N.N. Nikolaev, and S. Fantoni, Phys. Rev. Lett. 74 (1995) 3565
- [18] F. Low, Phys. Rev. D12 (1975) 163; S. Nussinov, Phys. Rev. Lett. 34 (1975) 1286; J.F. Gunion and D. Soper, Phys. Rev. D15 (1977) 2617
- [19] S.J. Brodsky and G.P. Lepage, Phys. Rev. D22 (1980) 2157
- [20] S.J. Brodsky et al., erratum Phys. Rev. D in print
- [21] B. Blättel, G. Baym, L.L. Frankfurt, and M. Strikman, Phys. Rev. Lett. 71 (1993) 896
- [22] L.L. Frankfurt, G.A. Miller, and M. Strikman, Phys. Lett. B304 (1993) 1
- [23] A. Mueller, Nucl. Phys. B335 (1990) 115
- [24] E.M. Levin and M.G. Ryskin, Sov. J. Nucl. Phys. 45 (1987) 150
- [25] J. Collins, L.L. Frankfurt, and M. Strikman in preparation
- [26] H. Cheng and T.T. Wu, Expanding Protons: Scattering at High Energies (MIT Press, Cambridge, Massachusetts, and London, England) Section 9 (1987)
- [27] M. Glück, E. Reya, and A. Vogt, Preprint DESY 94-206 (1994)
- [28] N.N. Nikolaev and B.G. Zakharov, Phys. Lett. B332 (1994) 184
- [29] A. Martin, Phys. Lett. 93B (1980) 338
- [30] C. Quigg and J.L. Rosner, Phys. Lett. 71B (1977) 153
- [31] V.L. Chernyak and A.R. Zhitnitski, Phys. Rep. 112 (1984) 173
- [32] NMC Collaboration, P. Amaudruz et al., Z. Phys. C51 (1991) 387; M. Arneodo et al., CERN-PRE/94-146
- [33] J.D. Bjorken, in Proceedings of the Fifth International Symposium on Electron and

- Photon Interactions at High Energies, Ithaca, New York, 1971, ed. N.B. Mistry (Cornell University Press, Ithaca, 1971), pp. 281-297; J.D Bjorken and J.B. Kogut, Phys. Rev. D8 (1973) 1341
- [34] L.L. Frankfurt, W. Koepf, and M. Strikman, work in progress.
- [35] L.L. Frankfurt, W. Koepf, and M. Strikman, Preprint hep-ph/9509311 (1995)
- [36] S.J. Brodsky (1994) and V. Gribov (1996), private communications to L.F.
- [37] W. Buchmüller and S.-H.H. Tye, Phys. Rev. D24 (1981) 132
- [38] M.G. Ryskin, R.G. Roberts, A.D. Martin, and E.M. Levin, Preprint RAL-TR-95-065 (1995)
- [39] H. Jung, D. Krücker, C. Greub, and D. Wyler, Z. Phys. C60 (1993) 721
- [40] A. Donnachie and P.V. Landshoff, Phys. Lett. B185 (1987) 403; Nucl. Phys. B311 (1989) 509
- [41] T.H. Bauer, R.D. Spital, D.R. Yennie, and F.M. Pipkin, Rev. Mod. Phys. 50 (1978) 261
- [42] A.D. Martin, W.J. Stirling, and R.G. Roberts, Preprint RAL-95-021 (1995)
- [43] H.L. Lai et al. (CTEQ Collaboration), Preprint MSU-HEP-41024 (1994)
- [44] M. Burkardt, J.M. Grandy, and J.W. Negele, Ann. Phys. 238 (1995) 441
- [45] E.V. Shuryak, Rev. Mod. Phys. 65 (1993) 281
- [46] Review of Particle Properties, Phys. Rev. D50 (1994) 1177
- [47] A.B.Clegg and A.Donnachie, Z. Phys. C62 (1994) 455
- [48] L.L. Frankfurt and M. Strikman, Nucl. Phys. B250 (1985) 147
- [49] T.J. Chapin et al., Phys.Rev. D31 (1985) 17

- [50] L.L.Frankfurt and M.I. Strikman, *Progr. Part. Nucl. Phys.*, 27, (1991) 135
- [51] N.N. Nikolaev and B.G. Zakharov, *Z. Phys.* C64 (1994) 631
- [52] V. Barone, M. Genovese, N.N. Nikolaev, E. Predazzi, and B.G. Zakharov, *Phys. Lett.* B326 (1994) 161
- [53] V.Abramovskii, V. N. Gribov, and O. V. Kancheli, *Sov. J. Nucl. Phys.* 18, (1974) 308
- [54] B. Badelek, M. Krawczyk, K. Charchula, J.Kwiecinski, *Rev. Mod. Phys.* 64 (1992) 927
- [55] E. Laenen and E. Levin, *Ann. Rev. Nucl. Part. Sci.* 44 (1994) 199
- [56] J. Collins and J. Kwiecinski, *Nucl. Phys.* B335 (1990) 89
- [57] L.V. Gribov, E.M. Levin, M. G. Ryskin, *Phys. Rep.* 100 (1983) 1
- [58] A.H. Mueller and J. Qiu, *Nucl. Phys.* B268 (1986) 427
- [59] A.J. Askew, J. Kwiecinski, A.D. Martin, and P.J. Sutton, *Phys. Rev.* D49 (1994) 4440
- [60] R.J. Glauber, *Lectures in Theoretical Physics*, vol. 1, ed. W.E. Brittin et al., Interscience Publ., N.Y. (1959), p. 315
- [61] V.N. Gribov, *Sov. Phys. JETP* 29 (1969) 483
- [62] Jian-wei Qiu, *Nucl. Phys.* B291 (1987) 746
- [63] L.L. Frankfurt, M. Strikman, and S. Liuti, *Phys. Rev. Lett.* 65 (1990) 1725
- [64] K.J. Eskola, *Nucl. Phys.* B400 (1993) 240
- [65] K.J. Eskola, Jian-wei Qiu, and Xin-Nian Wang *Phys. Rev. Lett.* 72 (1994) 36
- [66] L.L. Frankfurt, M. Strikman, and S. Liuti, *Proceedings of PANIC XIII*, p.342 (1993), Ed. A. Pascolini, World Scientific (1993)
- [67] N.N. Nikolaev and B.G. Zakharov, *Z. Phys.* C49 (1991) 607

[68] L.L. Frankfurt, W. Koepf, and M. Strikman, work in progress.

[69] Xin-Nian Wang and M. Gyulassy, Phys. Rev. Lett. 68 (1992) 1480